

ESD-TDR-65-274

ESTI FILE COPY

ESD-TDR-65-274

ESD ACCESSION LIST

ESTI Call No. DL 47190

Copy No. 1 of 1 cys.

ESD RECORD COPY

RETURN TO
SCIENTIFIC & TECHNICAL INFORMATION DIVISION
(ESTI), BUILDING 1211

Technical Note

1965-28

B. F. LaPage

Some Properties of a Scanned Circular Array

7 July 1965

Prepared under Electronic Systems Division Contract AF 19 (628)-5167 by

Lincoln Laboratory

MASSACHUSETTS INSTITUTE OF TECHNOLOGY

Lexington, Massachusetts



ESPL

A0620460

The work reported in this document was performed at Lincoln Laboratory, a center for research operated by Massachusetts Institute of Technology, with the support of the U.S. Air Force under Contract AF 19(628)-5167.

MASSACHUSETTS INSTITUTE OF TECHNOLOGY
LINCOLN LABORATORY

SOME PROPERTIES OF A SCANNED CIRCULAR ARRAY

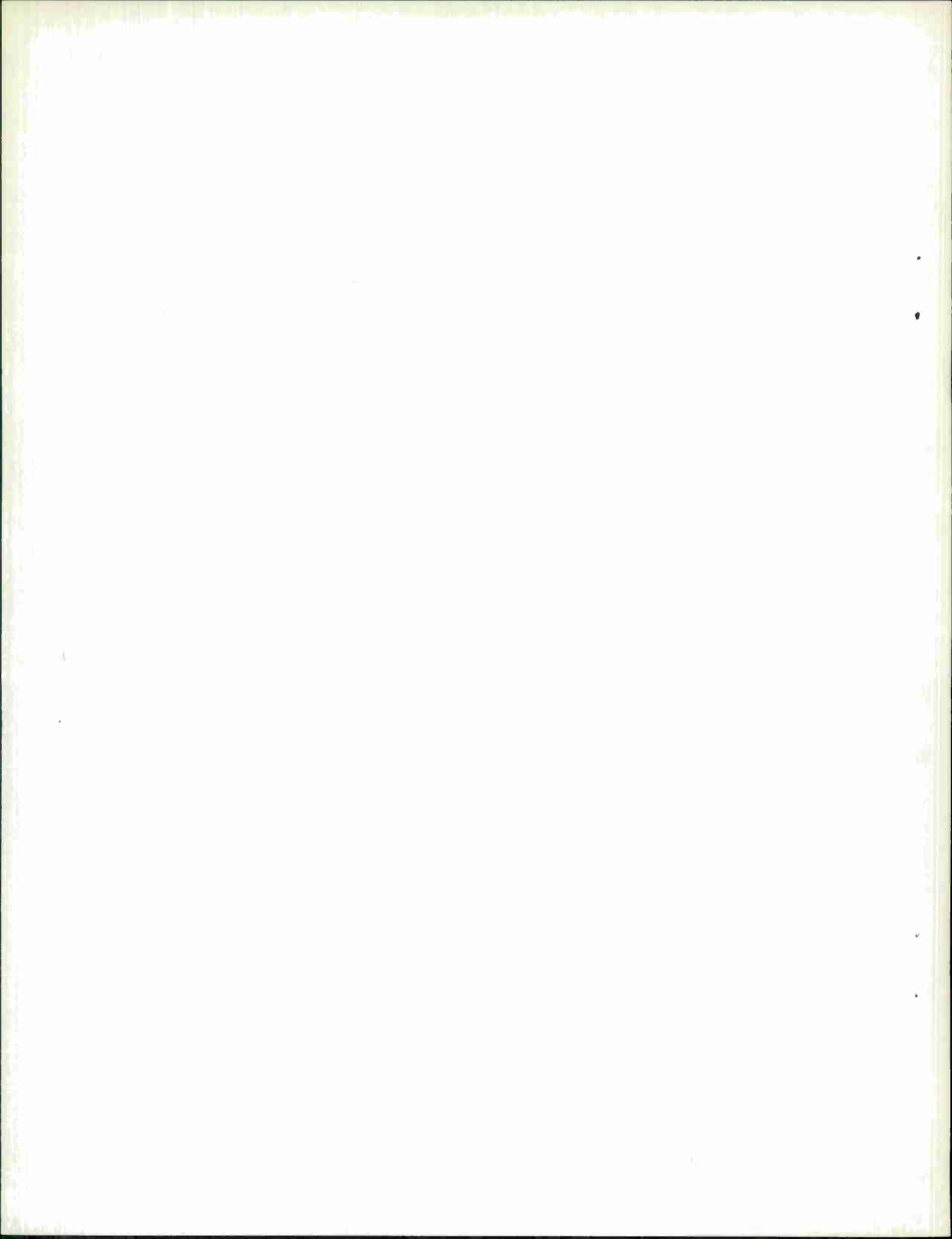
B. F. LaPAGE

Group 61

*ESEP Checked for
Public Release OK, LTH
17 Sept 65
Wrench*

TECHNICAL NOTE 1965-28

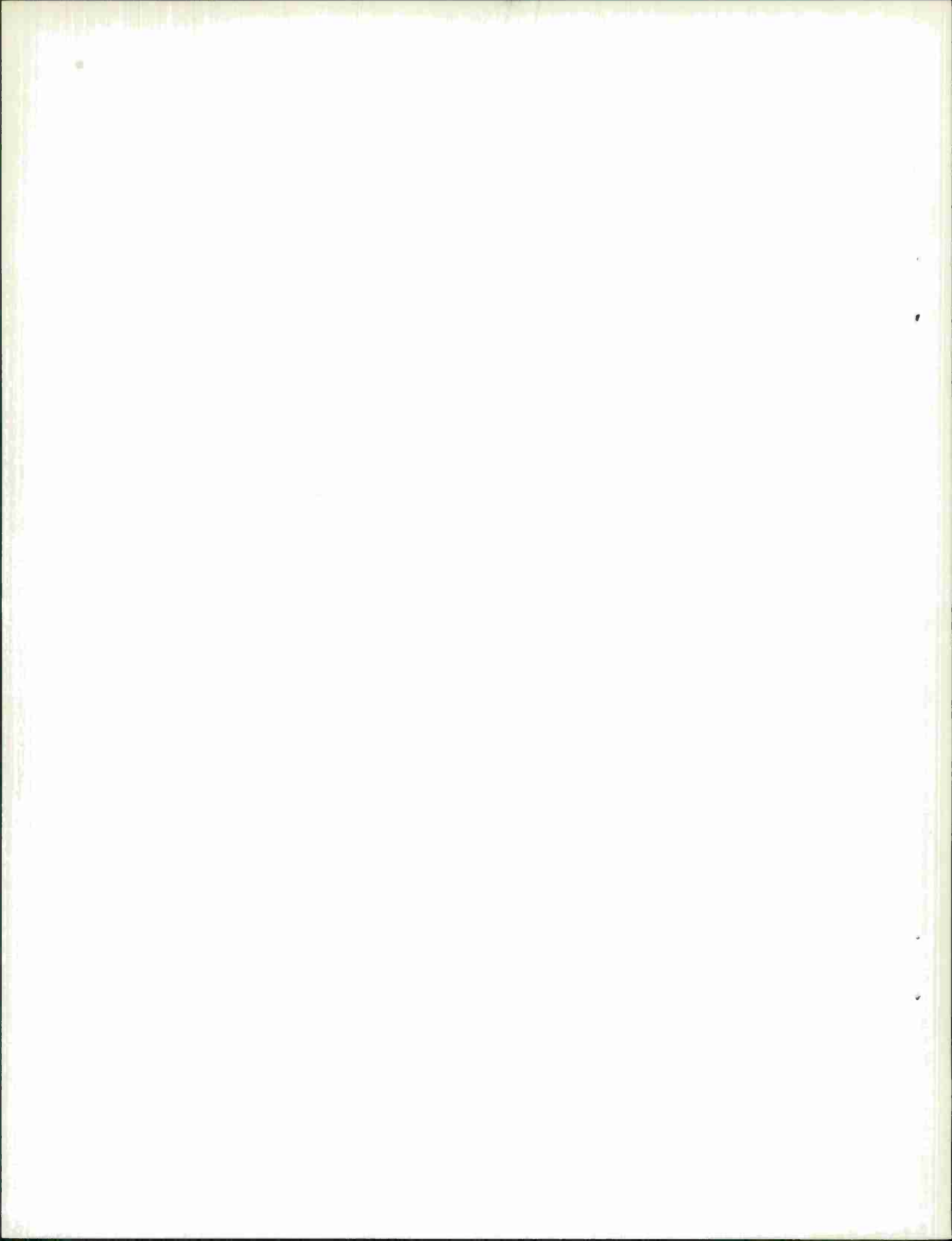
7 JULY 1965



ABSTRACT

The impedance, pattern and gain properties of a circular array of dipoles (or isotropic sources) is discussed. In particular the variation of these properties as the antenna beam is scanned is investigated. Computed results for typical arrays are shown and the meaning of the results are discussed, and further areas of investigation are indicated.

Accepted for the Air Force
Stanley J. Wisniewski
Lt Colonel, USAF
Chief, Lincoln Laboratory Office



Some Properties of a Scanned Circular Array

It has been proposed that a useful satellite antenna design could be achieved by using a circular array of monopoles located about the spin axis of a short cylinder as shown in Fig. 1. The spin axis of the satellite is oriented normal to the orbital plane and the antenna beam is "de-spun" by proper phasing of the currents on the array elements. The array elements are fed in pairs with equal amplitude currents from separate sources, and phased to produce the desired beam positions. A retro-directive scheme could also be used, but in any event some basic data was needed on the behavior of scanned circular arrays and this was the motivation of this study.

There is a fair amount of literature on the subject of circular arrays; notably Knudsen's¹ exhaustive study and more recently the work of Neff,² Simpson³ and Mack.⁴ Unfortunately, these studies are concerned with equi-phased arrays, parasitic array systems, or other types which are not directly applicable to our problem. The problem of the input impedance variations of an element during scan and the array gain variations are also not covered, and these topics are our main interest.

The gross parameters of the array were chosen⁵ from what was considered to be a reasonable size satellite based on total weight, solar cell output, booster capabilities, etc; and are typical, at least, for the near future.

The geometry of the array that is under discussion is shown in Fig. 2.

The N-elements are arranged on a circle of radius a, located in the x-y plane and phased to point the resultant beam at an angle ϕ_0 ($\theta_0 = 90^\circ$). Each element is positioned by the angle coordinate ϕ_n where

$$\phi_n = \frac{2\pi}{N} (n - 1) \quad (1)$$

The current on the i^{th} element is given by

$$I_i = e^{j\psi_i}, \quad |I_i| = 1 \quad (2)$$

where

$$\psi_i = -ka \cos(\phi_0 - \phi_n)$$

Now the field due to the i^{th} element is

$$E_i = e^{j[\psi_i + ka \cos(\phi - \phi_n)]} \quad (3)$$

or

$$E_i = e^{jka[\cos(\phi - \phi_n) - \cos(\phi_0 - \phi_n)]}$$

The total field is obtained by summing all E_i , or

$$E(\phi) = \sum_{n=1}^N e^{jka[\cos(\phi - \phi_n) - \cos(\phi_0 - \phi_n)]} \quad (4)$$

This can be written in the equivalent form as

$$E(\phi) = \sum_{n=1}^N e^{j u \sin \alpha_n} , \quad (5)$$

$$\alpha_n = \phi_n - \frac{\phi + \phi_0}{2}$$

$$u = 2ka \sin \frac{\phi - \phi_0}{2} .$$

We see from Eq. (4) that when $\phi_0 = \phi_n$, or the beam points to an element position angle, $E(\phi)$ does not depend on ϕ_0 . This means that any variations that occur in $E(\phi)$ have a periodicity of the inter-element angular spacing, and we need to study only half that interval to obtain all the scan pattern variations. Now Eq. (5) may be transformed by using Bessel's expansion:

$$e^{jZ \sin \theta} = \sum_{n=-\infty}^{\infty} e^{jn\theta} J_n(Z) , \quad (6)$$

putting the result in a form, that is for large N , easier to analyze. That is,

$$E(\phi) \simeq J_0(u) + 2J_N(u) \cos \frac{N}{2} (\phi + \phi_0), \quad N \text{ even} \quad (7)$$

$$E(\phi) \simeq J_0(u) - 2jJ_N(u) \sin \frac{N}{2} (\phi + \phi_0), \quad N \text{ odd} \quad (8)$$

$$u = 2ka \sin \frac{\phi - \phi_0}{2} .$$

Now we show that for $N \geq 6$, $E(\phi)$ is independent of N to a large degree. At

the null of $E(\phi)$ we have $J_0(x) = 0$ for $x = 2.404$ and $J_5(2.404) = .016$,
 $J_6(2.404) = .0033$, etc.

So it is evident that terms containing $J_6(u)$ are negligible, at least at the null of $E(\phi)$. We can say that for $N \geq 6$ all the array patterns null at nearly the same angle, given by

$$u_0 = 2ka \sin \frac{\phi}{2} = 2.404 \quad .$$

The 3 db beamwidth can be computed similarly, i. e.,

$$(BW_3)_0 = 4 \sin^{-1} \left(\frac{1.13}{2ka} \right) \quad .$$

Also, the first side lobe will have a level of -7.9 db located at an angle

$$(SL_\theta)_0 = 2 \sin^{-1} \left(\frac{3.83}{2ka} \right) \quad .$$

We can now give the array plane pattern for all ring arrays with $N \geq 6$, as shown in Fig. 3. For $N = 4, 5$ the beamwidth and null position will be nearly the same as in Fig. 3 but the side lobe level will be completely different. It should be noted that the condition $u \leq 2ka$ is necessary for ϕ to be real, and hence the pattern to be in the visible region. The pattern of the array in the plane normal to the array plane, for isotropic sources, can be analyzed in a similar manner to obtain the result

$$E(\theta, \phi_0) \simeq J_0(u) + J_N(u) \begin{cases} 2 \cos N \left(\frac{\pi}{2} + \phi_0 \right) & N \text{ even} \\ 2j \sin N \left(\frac{\pi}{2} + \phi_0 \right) & N \text{ odd} \end{cases} \quad (9)$$

$$u = ka (\sin \theta - 1) \quad .$$

This is the same form previously given except for a change in the argument of $J_0(u)$. One might ask — how can we get directivity in a plane orthogonal to the array plane for isotropic sources? The answer is seen when one "collapses" the point sources along a line and it is observed that we have an end fire array with tapered amplitude distribution. This is known to produce two-plane directivity; the well known Yagi antenna being an example of this principle. Of course, if array elements such as dipoles are considered, then the array pattern must be modified to take into account the element pattern. Figures 4 and 5 show the array 3 db beamwidth vs. array diameter (ka) for the "in-plane" and "out-of-plane" cases. We can now estimate the gain of the antenna array by using the well known expression

$$G \simeq \frac{27,000}{\theta_E^{\circ} \times \theta_H^{\circ}}$$

where θ_E° , θ_H° , are the principal plane half-power beamwidths, in degrees.

Using the data in Figs. 4 and 5 we get the result shown in Fig. 6 as a gain estimate. Notice that the gain given is referenced to the gain of an element.

These curves tell us that for a satellite of about 1λ diameter, we can expect beamwidths not less than 60° wide and total gains of 10 - 12 db over isotropic. (This assumes that monopoles are used and the top and bottom arrays are spaced 0.7λ .) More exact gain calculations presented later show that the gain estimates of Fig. 6 are quite good.

Equation (4) has been used to machine compute a series of patterns as a function of ka , N , ϕ , and scan angle ϕ_0 . The following combinations of values were used

$$\begin{aligned} Ka &= 2, 4, 6, 8, 10 & N &= 4, 6, 7, 8, 10 \\ k &= 0, .1, .2, .3, .4, .5, & 0 \leq \phi \leq 180^\circ, \Delta\phi &= 10^\circ \end{aligned}$$

k is a parameter that tells us where the beam is pointed, i. e. ,

$$\phi_0 = k\phi_n = k \frac{2\pi}{N}$$

A range of $0 \leq k \leq .5$ scans the beam one-half an inter-element angular spacing and this includes all the desired pattern data as mentioned before. Both in-plane and out-of-plane patterns were computed, but our main interest is in the array plane patterns. Some of this data is given in Fig. 7 (a through d). The patterns for $N \geq 6$ show the general characteristics for the main beam given by the approximate formulas, but as expected the side and back lobe levels are considerably different. The patterns for $N = 4$, $Ka = 2.28$ (Fig. 8) for example, show a back lobe for some scan angles whose intensity

Then

$$P_T = \sum_s |I_s|^2 R_e(Z_s)$$

and for a single element

$$P_o = |I_o|^2 R_e(Z_{oo})$$

The field intensities are related by

$$E_o = k |I_o|$$

$$E_T = \sum_s k |I_s| = k \sum_s |I_s|$$

Since the fields are "phased" to produce a maximum, the power gain is defined

as

$$G = \frac{|E_T|^2}{|E_o|^2} \text{ for } P_o = P_T$$

and we have

$$G = \frac{k^2 \left(\sum_s |I_s| \right)^2}{k^2 |I_o|^2} = \frac{R_e(Z_{oo}) \left(\sum_s |I_s| \right)^2}{\sum_s \{ |I_s|^2 R_e(Z_s) \}}$$

Now in our case $I_s = e^{j\phi_s}$, since $|I_s| = 1$.

Then

$$G = \frac{N^2 R_e(Z_{oo})}{\sum_s R_e(Z_s)} .$$

Since

$$R_e(Z_s) = \sum_j \left\{ |Z_{sj}| \cos(\alpha_{sj} + \phi_j - \phi_s) \right\}$$

where

$$\alpha_{sj} = \tan^{-1} \frac{X_{sj}}{R_{sj}}, \quad Z_{sj} = R_{sj} + jX_{sj} ,$$

ϕ_j = phase of the current in j^{th} element.

The final form of the gain expression is:

$$G \text{ (over an element)} = \frac{N^2 R_e(Z_{oo})}{\sum_{s=1}^N \sum_{j=1}^N \left\{ |Z_{sj}| \cos(\alpha_{sj} + \phi_j - \phi_s) \right\}} . \quad (11)$$

We also have the important relations:

$$Z_{oo} = Z_{ss} \quad (\text{identical elements}) ,$$

$$Z_{mn} = Z_{nm} \quad (\text{reciprocity of mutual impedance}) ,$$

$$\phi_i = ka \cos \frac{2\pi}{N} (p - i + 1) \quad (0 \leq p \leq \frac{1}{2} \text{ scan factor}) \quad .$$

Now Eq. (11) reduces to the form $G = N$ if all $Z_{mn} = 0$ for $m \neq n$, as it should. The formula also agrees exactly with some results given in Kraus⁶ for two elements spaced one-half wavelength, with in phase and out-of-phase excitations. In order to provide more flexibility, a separate computer subroutine is used to compute the mutual impedances, given the length of an element L/λ and the spacing d/λ . The induced EMF method⁷ is used, which assumes sinusoidal antenna currents and infinitely thin dipoles. The mutual impedance of parallel spaced dipoles can be expressed by using the Ci and Si functions,⁸ but for machine computation more effort is expended in calculating these functions than in a direct calculation of the mutual impedance itself. The input parameters to the main computer program are as follows:

<u>Parameter</u>	<u>Values Used</u>
N - number of elements	4, 5, 6
ka - ring size	2.28, 2.50, 2.75, 3.0
L/λ - dipole length, wavelengths	.475, .500, .525

The program computes the following:

1. All mutual impedances Z_{sj} .
2. All self impedances Z_{oo} .
3. Input impedance of each element vs. scan angle.

4. Gain of the array vs. scan angle.

A typical calculation result is shown in Fig. 10. The gain variation is seen to be very small. However, the input impedance variation is quite large. In fact, some combinations of parameters even lead to negative real values of input impedance. This indicates that more power is flowing towards the generator for that element, than away from it. An operating condition that one would certainly wish to avoid. To show the variations in a more readily understandable format, we have normalized the dipole input impedance values to 100 ohms and plotted them on a Smith Chart. This is equivalent to normalizing a monopole input impedance to a 50 ohm transmission line, a practical consideration in any actual system. Figures 11 (a through m) shows some typical data along with the gain variations and self impedance values. The impedance variation causes the VSWR to vary between 2 and 3. If we are willing to give up the continuous beam scanning in favor of a step-scanned system, we can avoid the ends of the impedance variations curve and reduce the variation to about a VSWR of 1.7. This step-scanning procedure causes discrete overlapping beams and a subsequent loss in gain under some conditions. For the $N = 6$ case, for instance, the stepping would be in 60° increments and would produce a 3.0 db ripple in the scanned pattern. Another possible way to minimize the impedance variation is to use isolators in each element feed line. A VSWR of 2.0 is effectively reduced to 1.23 for 10 db isolation loss and for 20 db loss the effective VSWR is 1.07. Recent advances

in the design of coaxial isolators has made available units that have 20 db reverse loss and 0.7 db forward loss and weigh less than one pound. These values are typical of commercial units and have not been optimized, especially as regards the weight of the unit, for satellite use.

It is the author's opinion that an analysis of the properties of a ring array of dipoles much more rigorous than that presented here is of little immediate value. The reason for this is that the mathematical model of monopoles on an infinite ground plane bears a questionable resemblance to monopoles arrayed on the top and bottom of a small cylinder. Until an exact analysis of the actual geometry is made and then checked with measured data, the correlation between model and real world is not really known. It is felt that a survey type look at a large number of possible satellite antenna schemes is more desirable, so that the most promising of these may receive more intensive scrutiny from the analytical and the experimental viewpoint.

Some computations concerned with the allowable tolerance on the excitation currents necessary to keep gain variations within some arbitrary bound have been made by the author, and the results are given in Lincoln Laboratory Technical Memorandum 61L-0016.

Mr. Robert Peck (Group 61) programmed the IBM-7094 for the computations given in this report.

REFERENCES

1. H. L. Knudsen, "Radiation from Ring Quasi-Arrays," Trans. IRE, PGAP AP-4, 452-472 (1956).
2. H. P. Neff and J. D. Tillman, "An Electronically Scanned Circular Antenna Array," IRE International Convention Record, Part I, 41-47 (1960).
3. T. L. Simpson and J. D. Tillman, "Parasitic Excitation of Circular Antenna Arrays," IRE, PGAP AP-9, 263-267 (1961).
4. R. B. Mack, "A Study of Circular Arrays," TR-381 and TR-386, Harvard University, Cruft Laboratory, Cambridge, Mass. (1963).
5. B. Reiffen, M. I. T., Lincoln Laboratory (private communication).
6. J. D. Kraus, Antennas (McGraw-Hill, New York, 1950) 283-292.
7. Ibid., 254-271.
8. Ibid., 265.

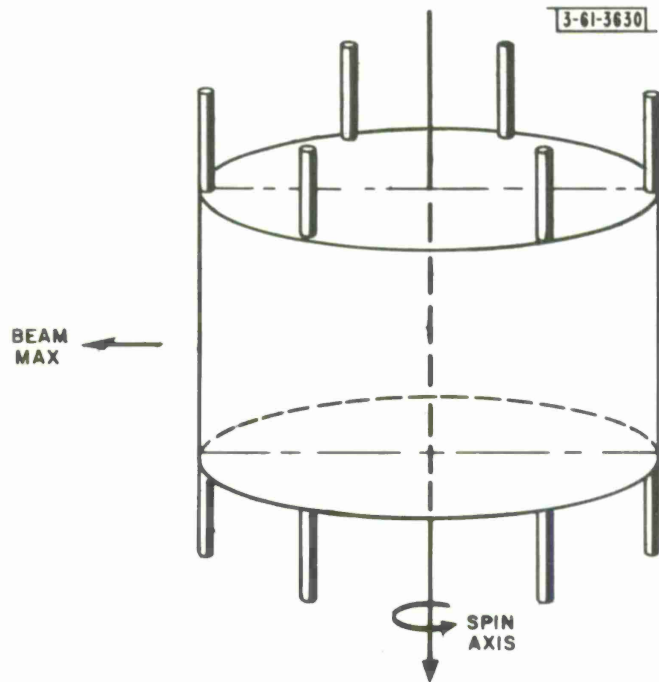


Fig. 1. Satellite antenna configuration.

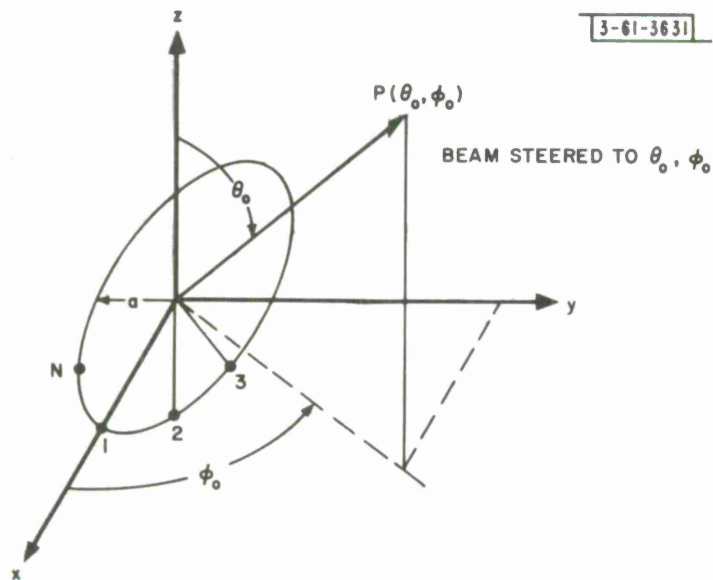


Fig. 2. Array geometry.

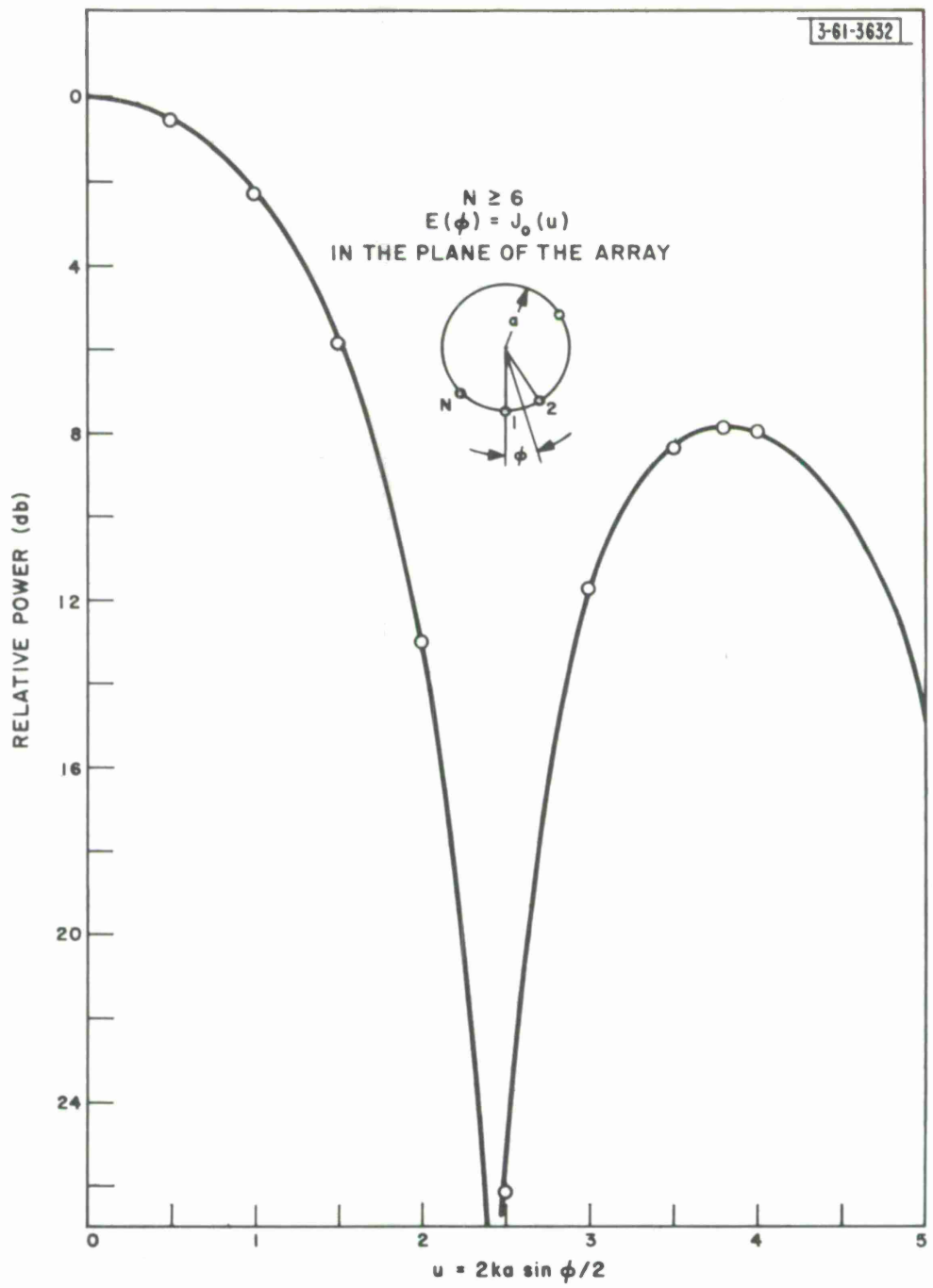


Fig. 3. Ring array pattern.

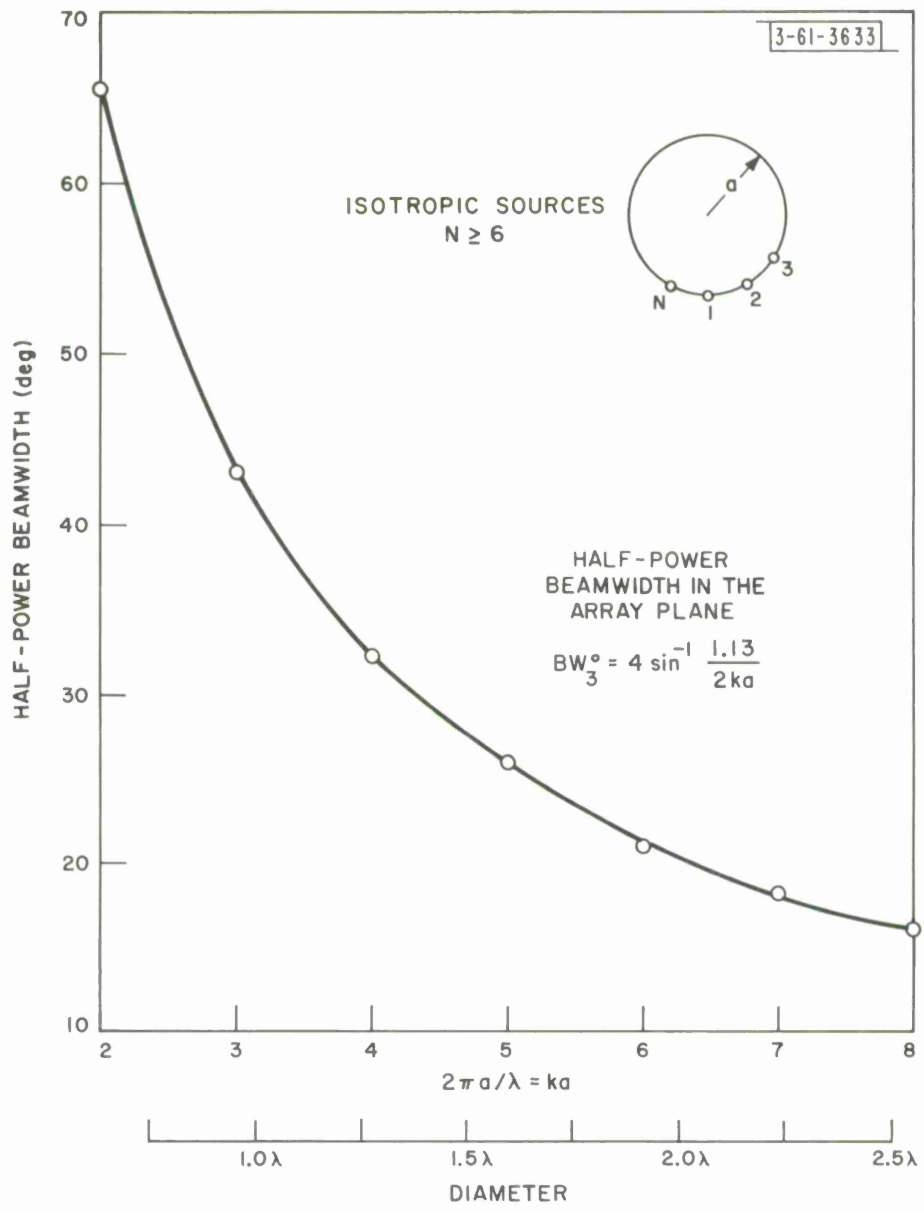


Fig. 4. Ring array beamwidth vs. diameter.

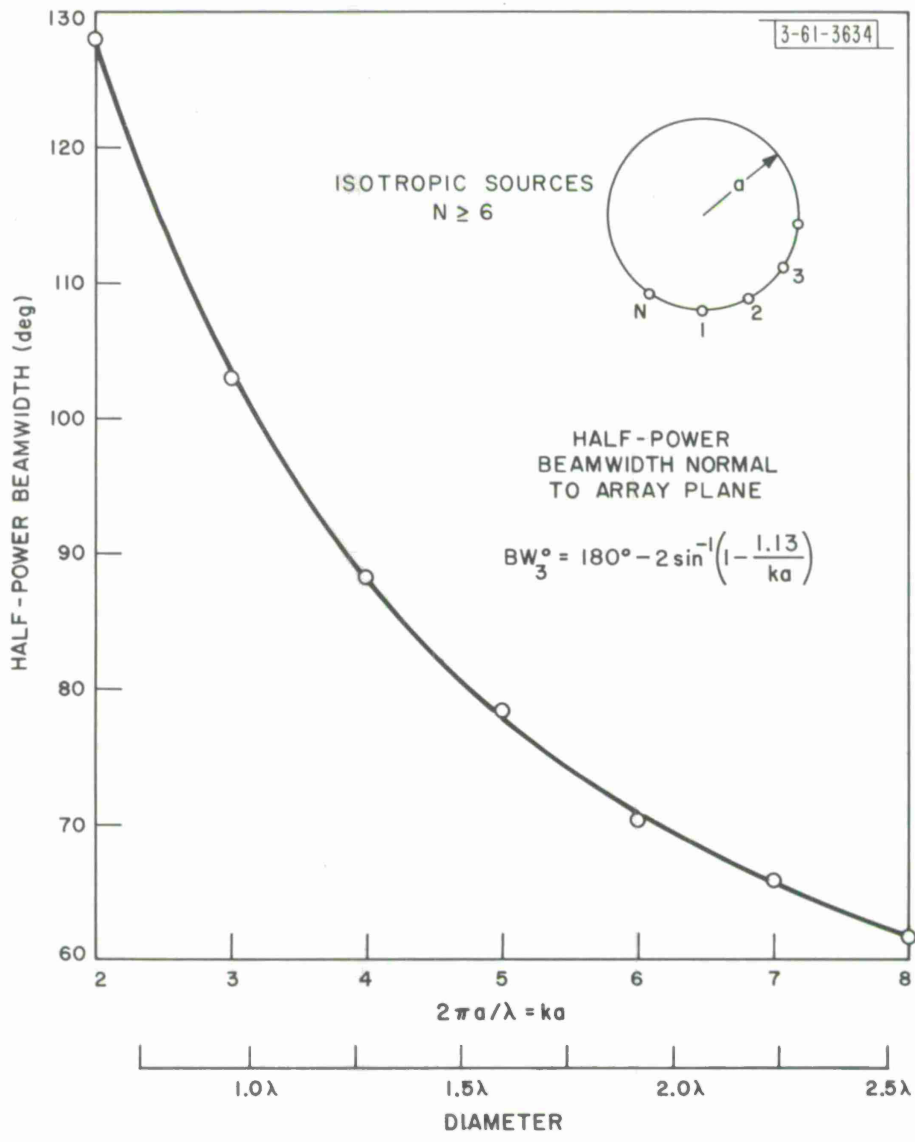


Fig. 5. Ring array beamwidth vs. diameter.

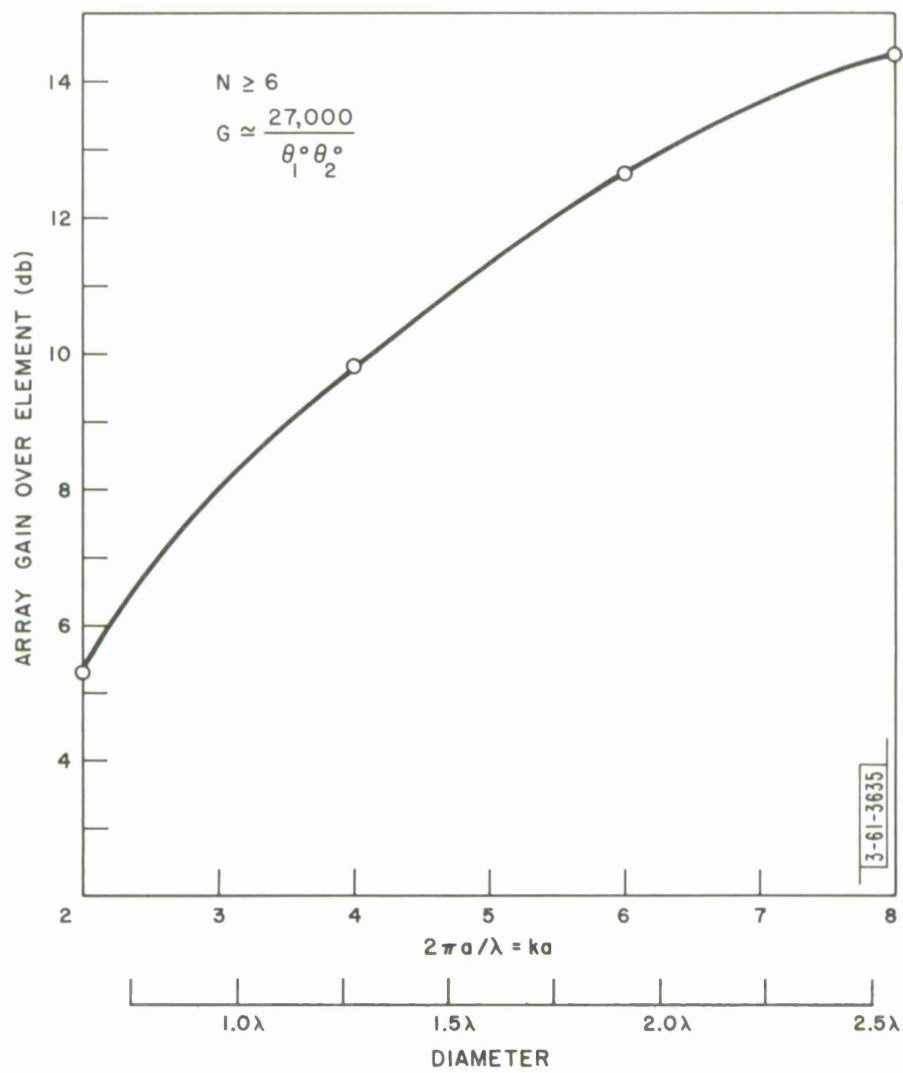


Fig. 6. Ring array gain vs. diameter.

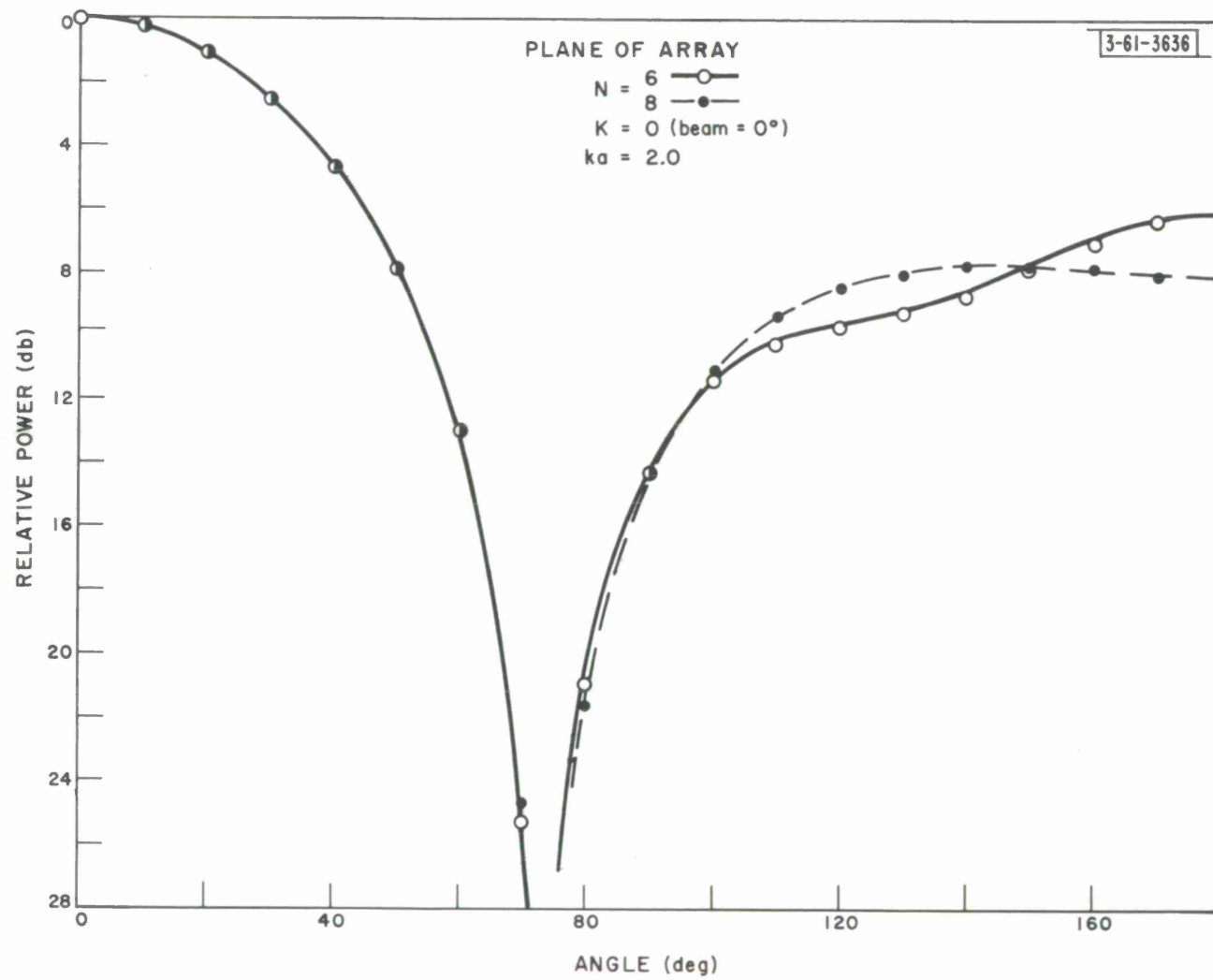


Fig. 7-a. Pattern of circular array.

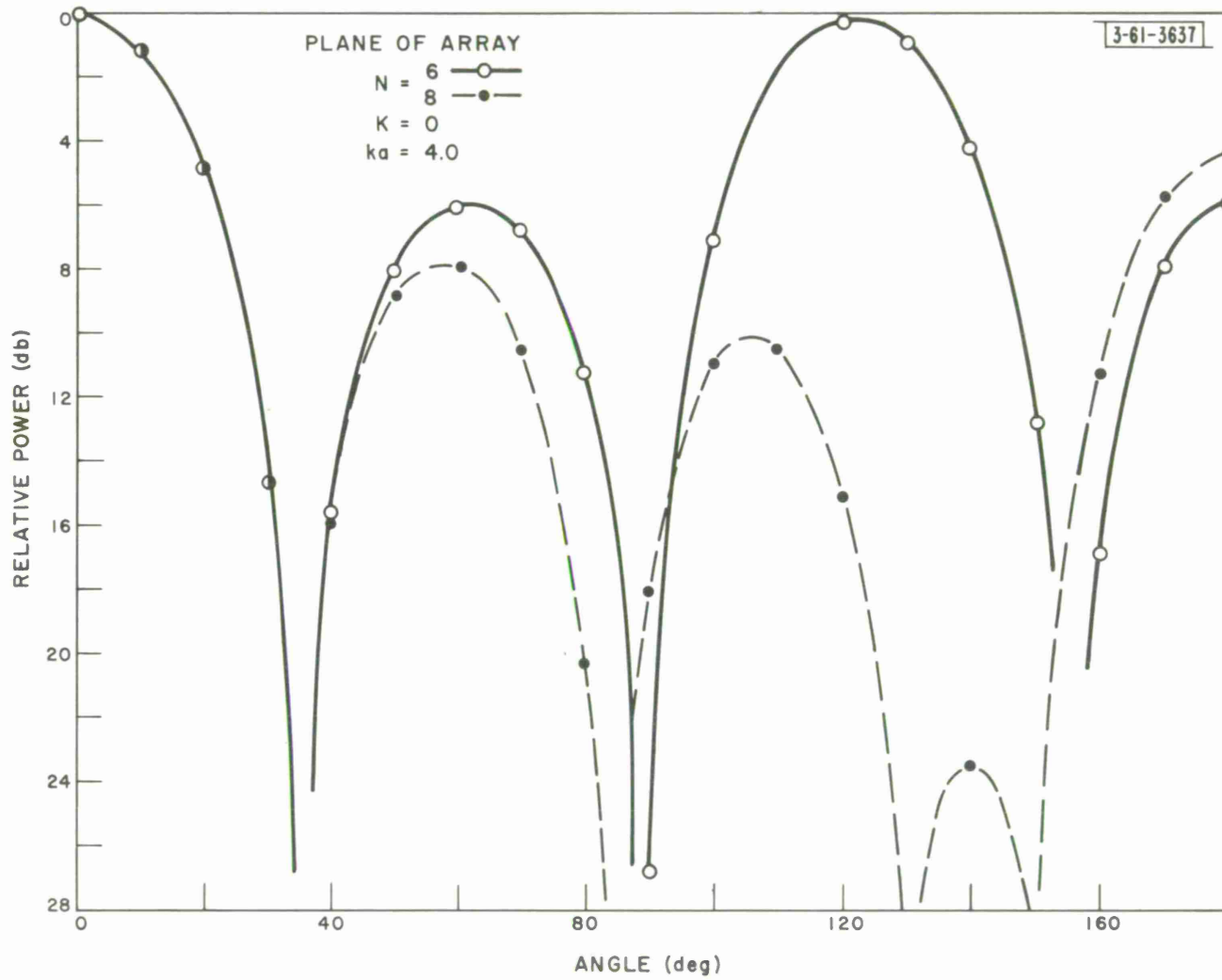


Fig. 7-b. Pattern of circular array.

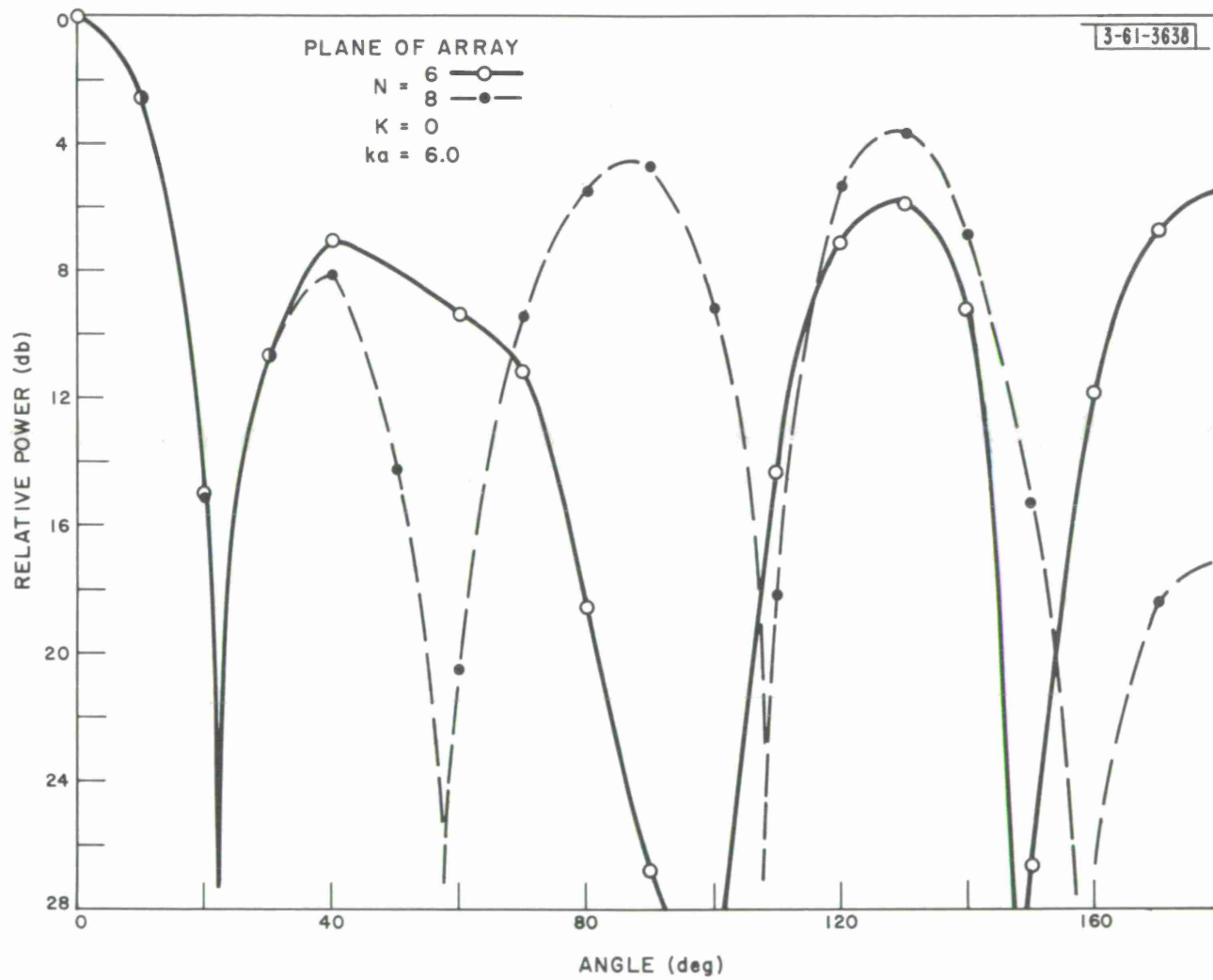


Fig. 7-c. Pattern of circular array.

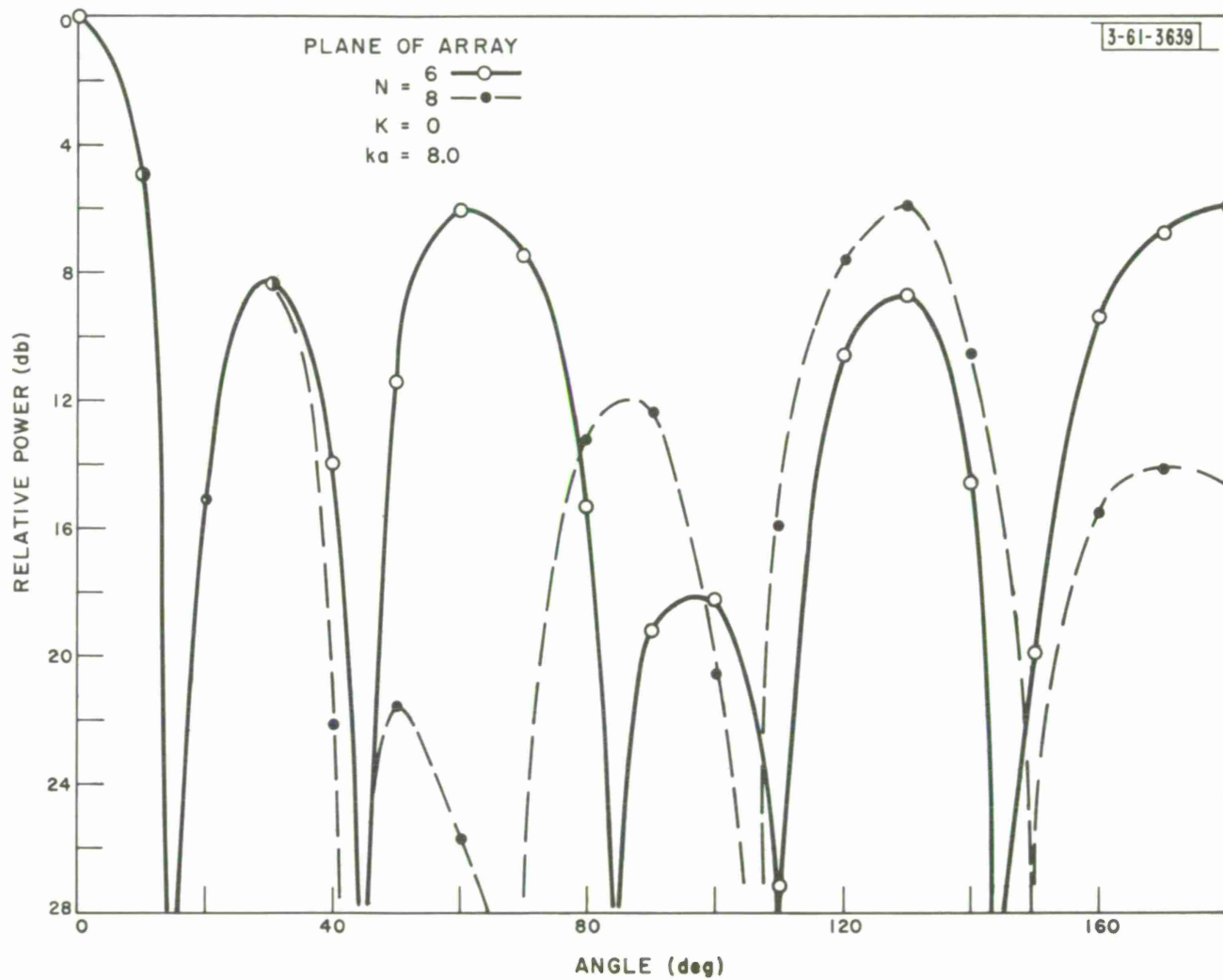


Fig. 7-d. Pattern of circular array.

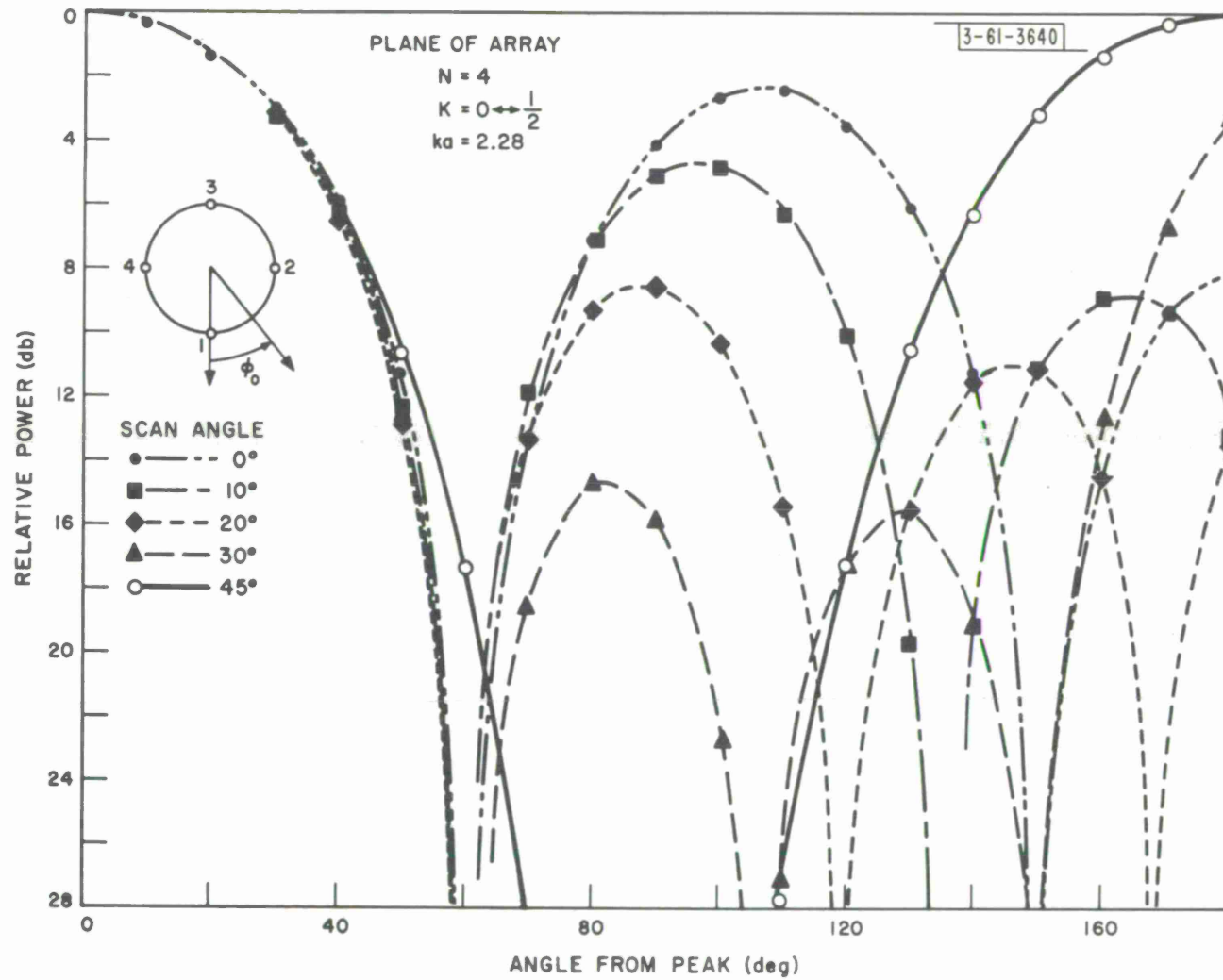


Fig. 8. Pattern of circular array.

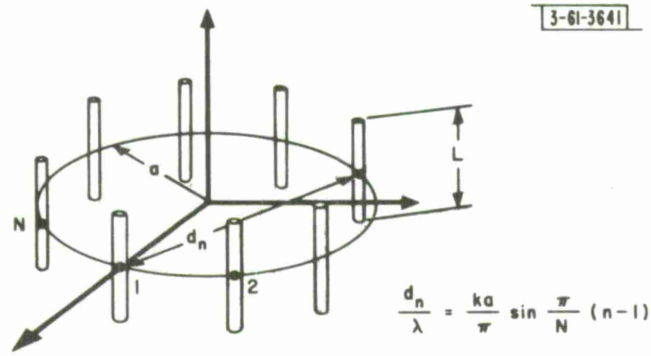


Fig. 9. Dipole array geometry.

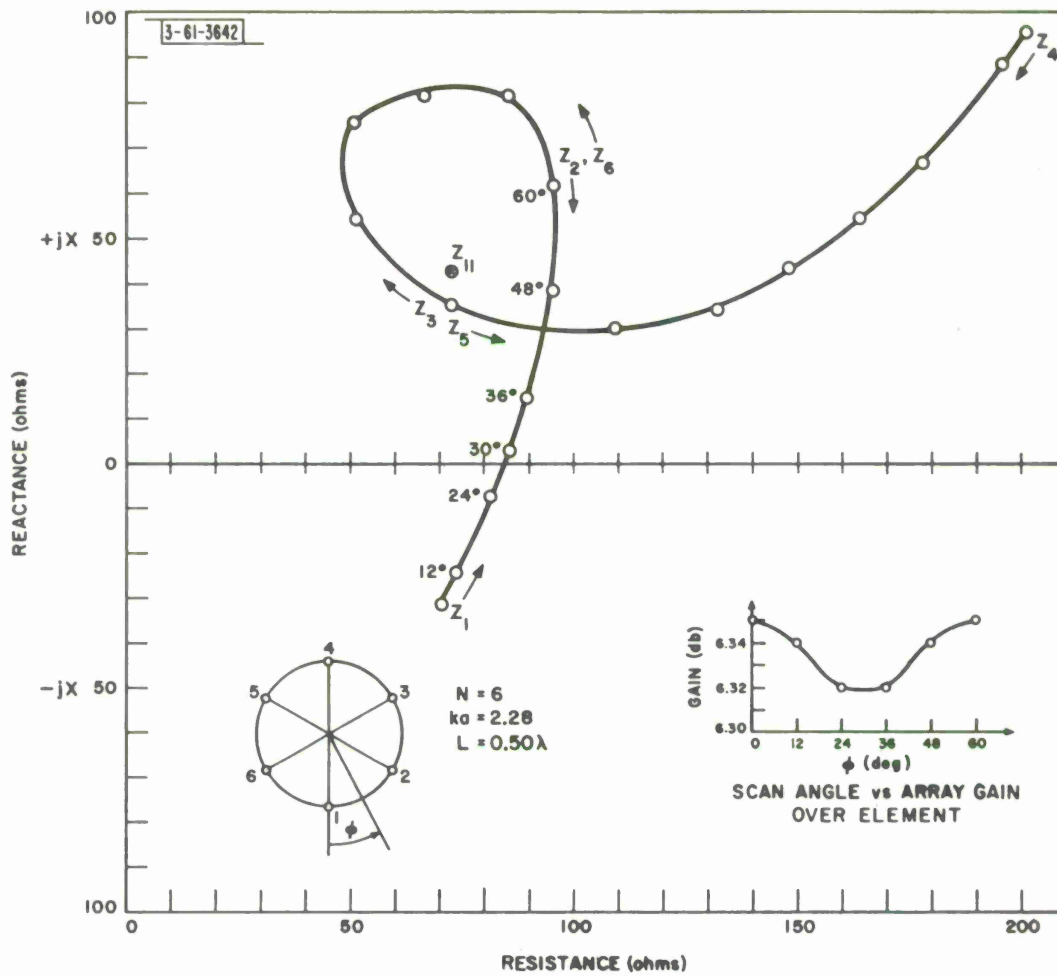


Fig. 10. Input impedance vs. scan angle.

$$Z_{II} = 73.1 + j42.5$$

3-61-3643

N = 6
ka = 2.28
L = 0.500

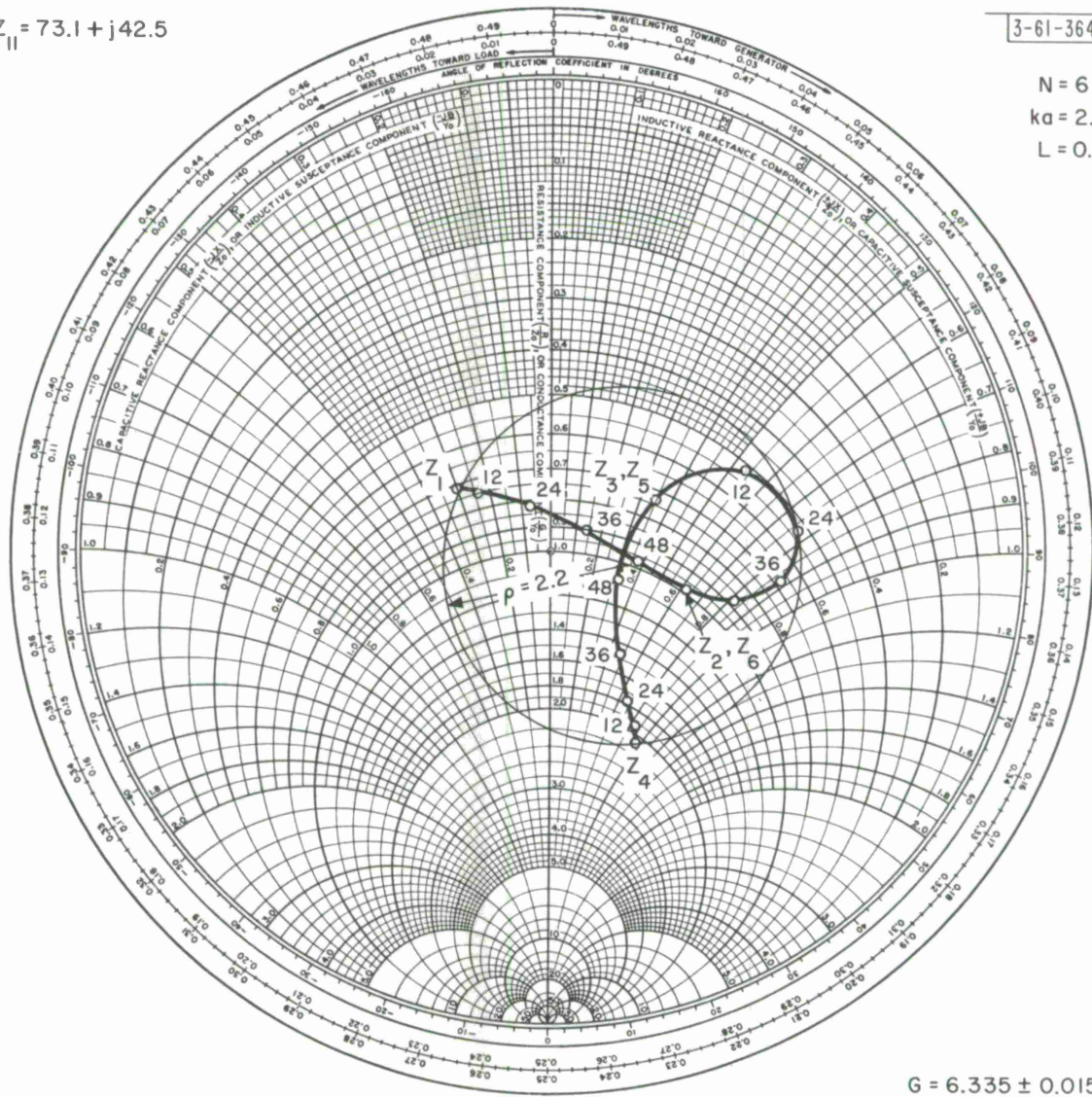
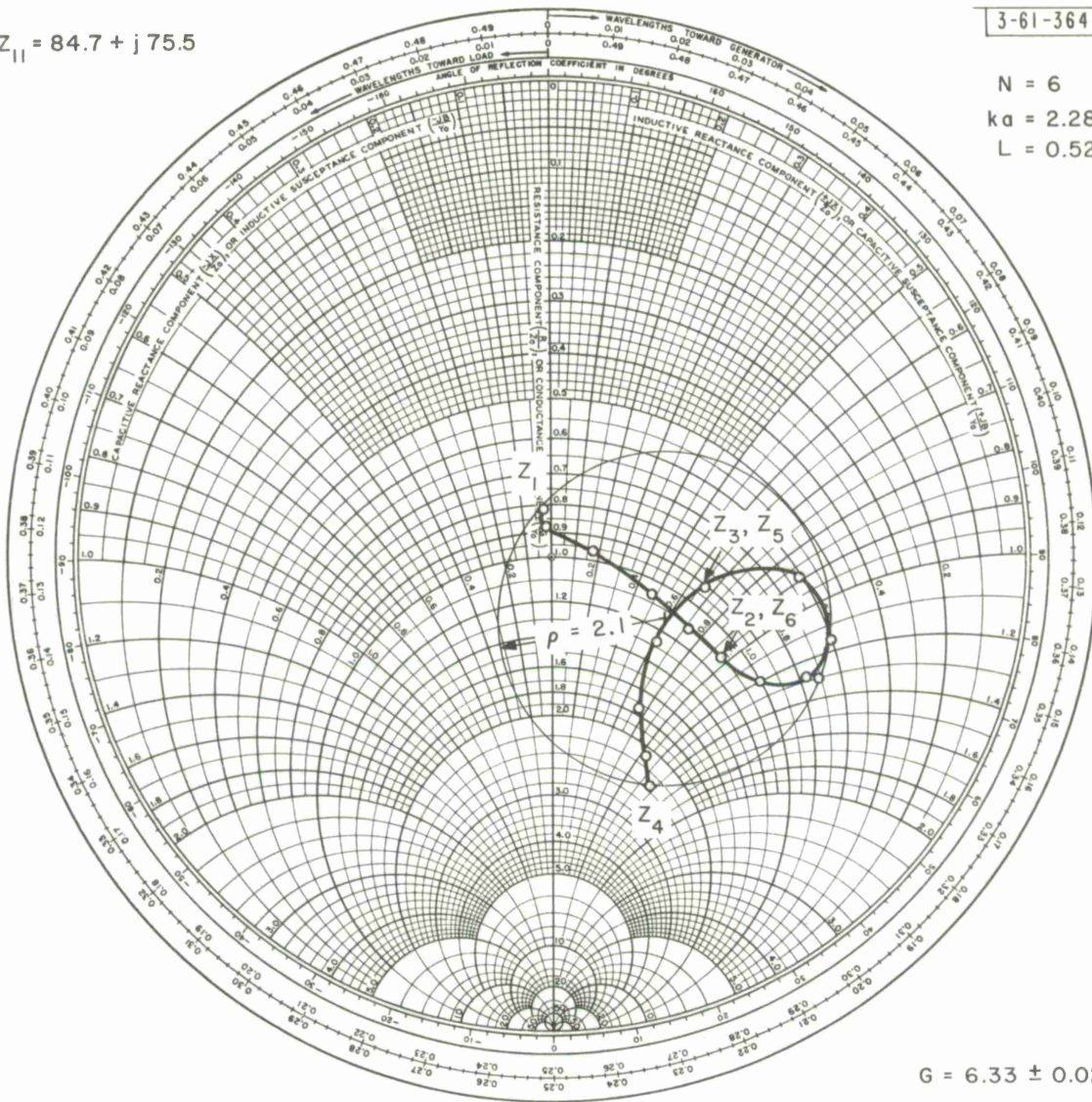


Fig. 11-a. Ring array impedance.

$$Z_{11} = 84.7 + j75.5$$

3-61-3644

N = 6
ka = 2.28
L = 0.525



G = 6.33 ± 0.02 db

Fig. 11-b. Ring array impedance.

$$Z = 63.1 + j10.4$$

3-61-3645

N = 6
 $ka = 2.28$
 $L = 0.475$

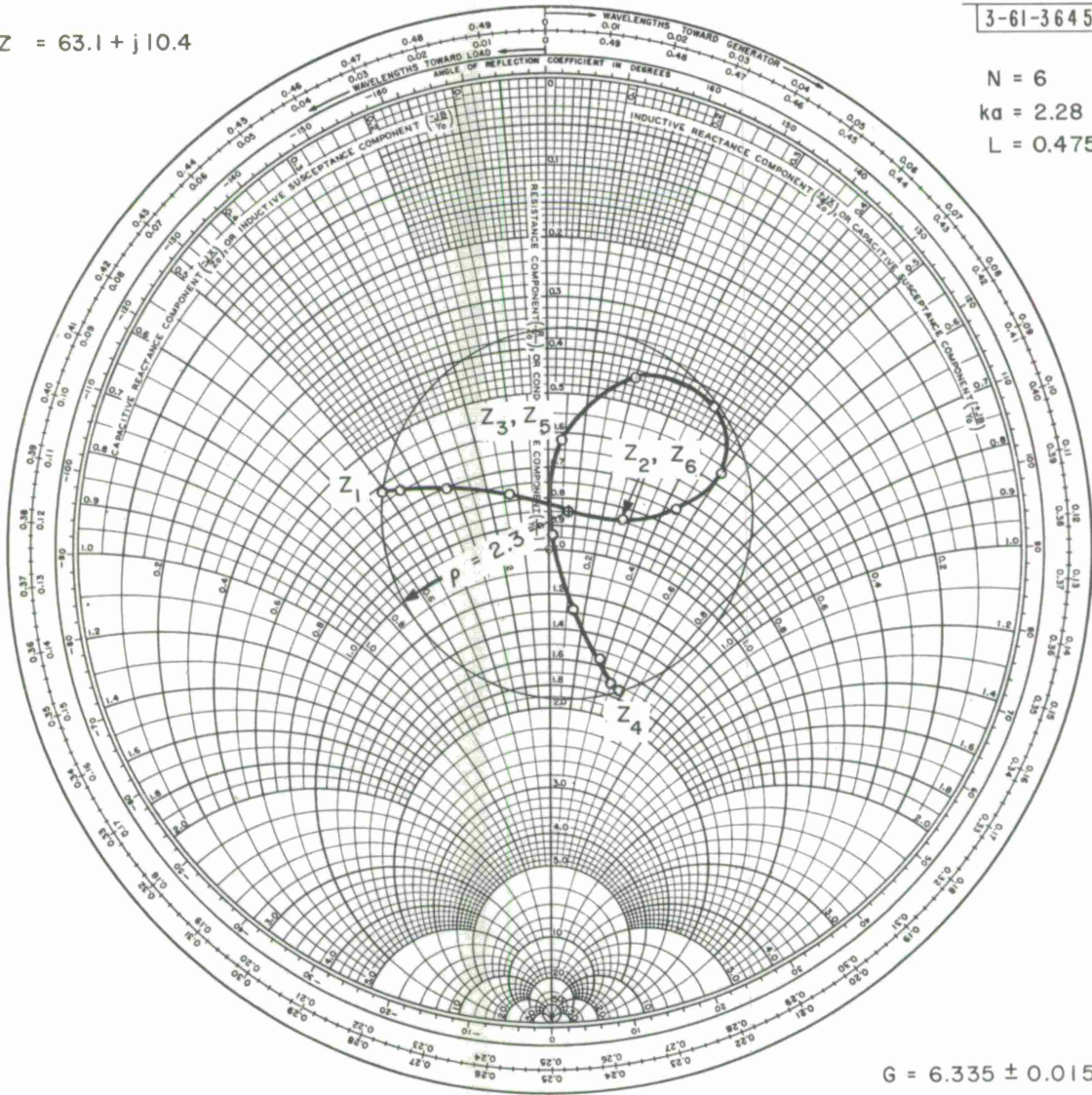


Fig. 11-c. Ring array impedance.

$$Z_{II} = 63.1 + j10.4$$

3-61-3646

N = 6
 ka = 2.50
 L = 0.475

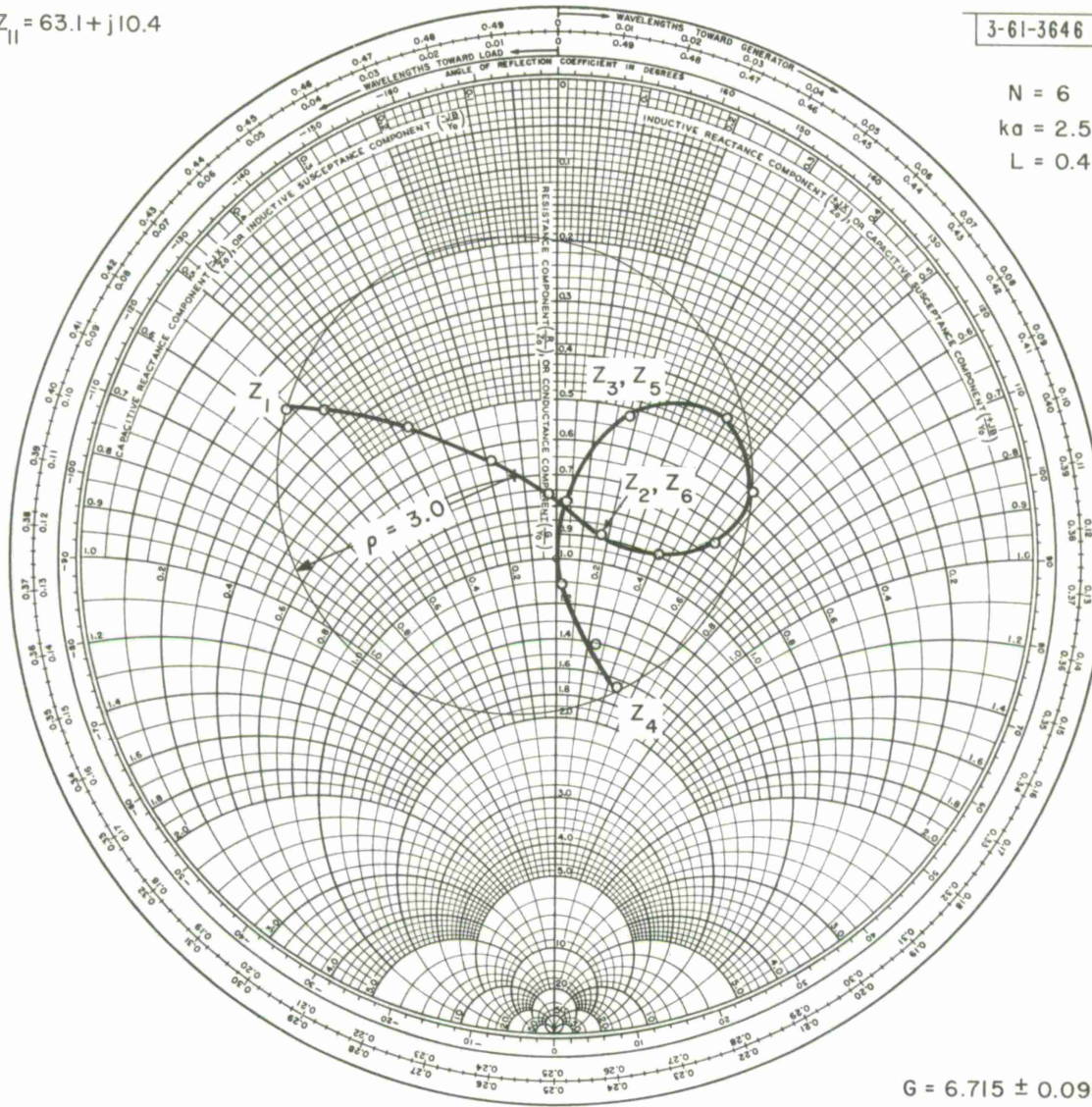
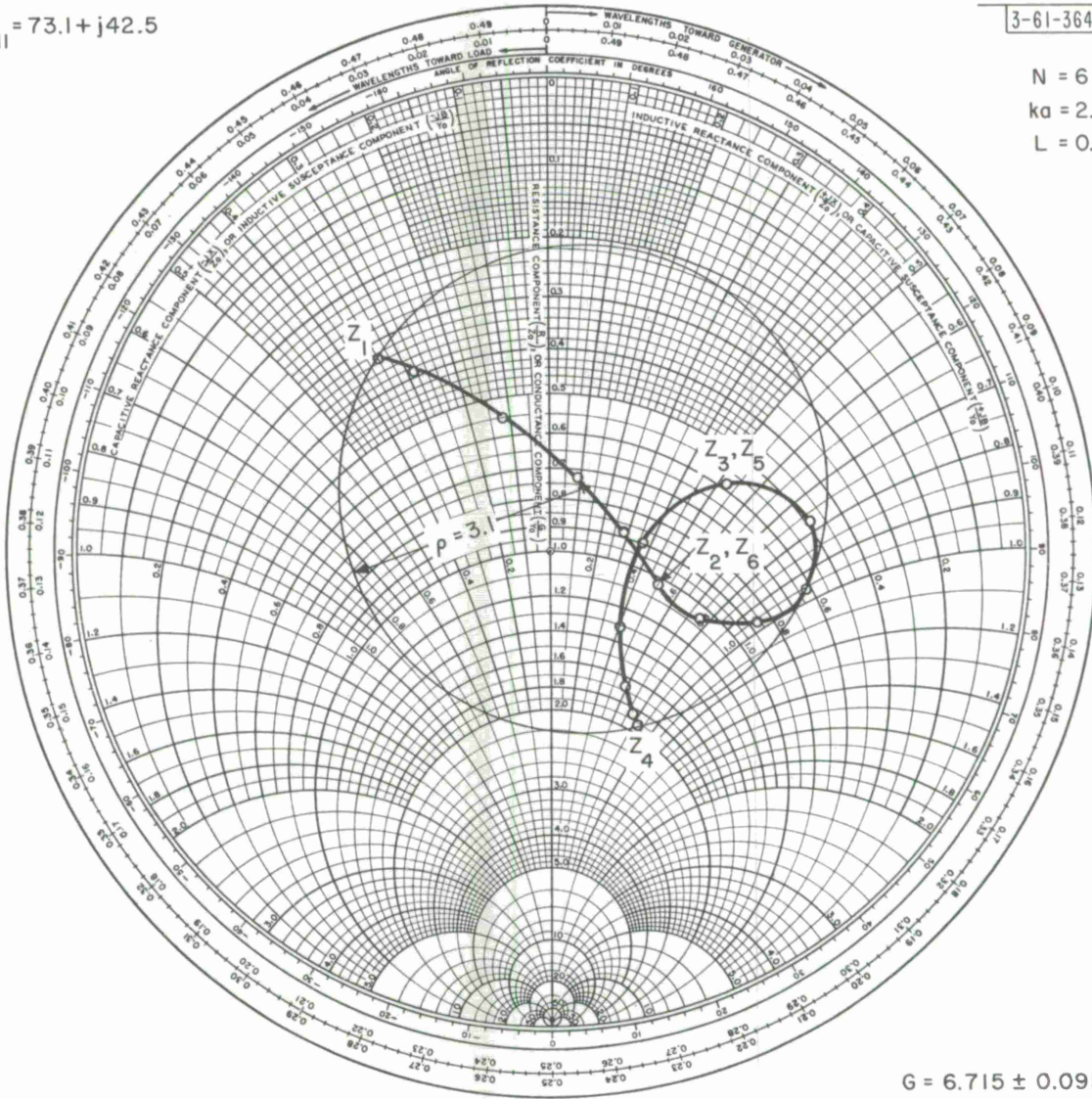


Fig. 11-d. Ring array impedance.

$$Z_{11} = 73.1 + j42.5$$

3-61-3647

N = 6
 ka = 2.50
 L = 0.500



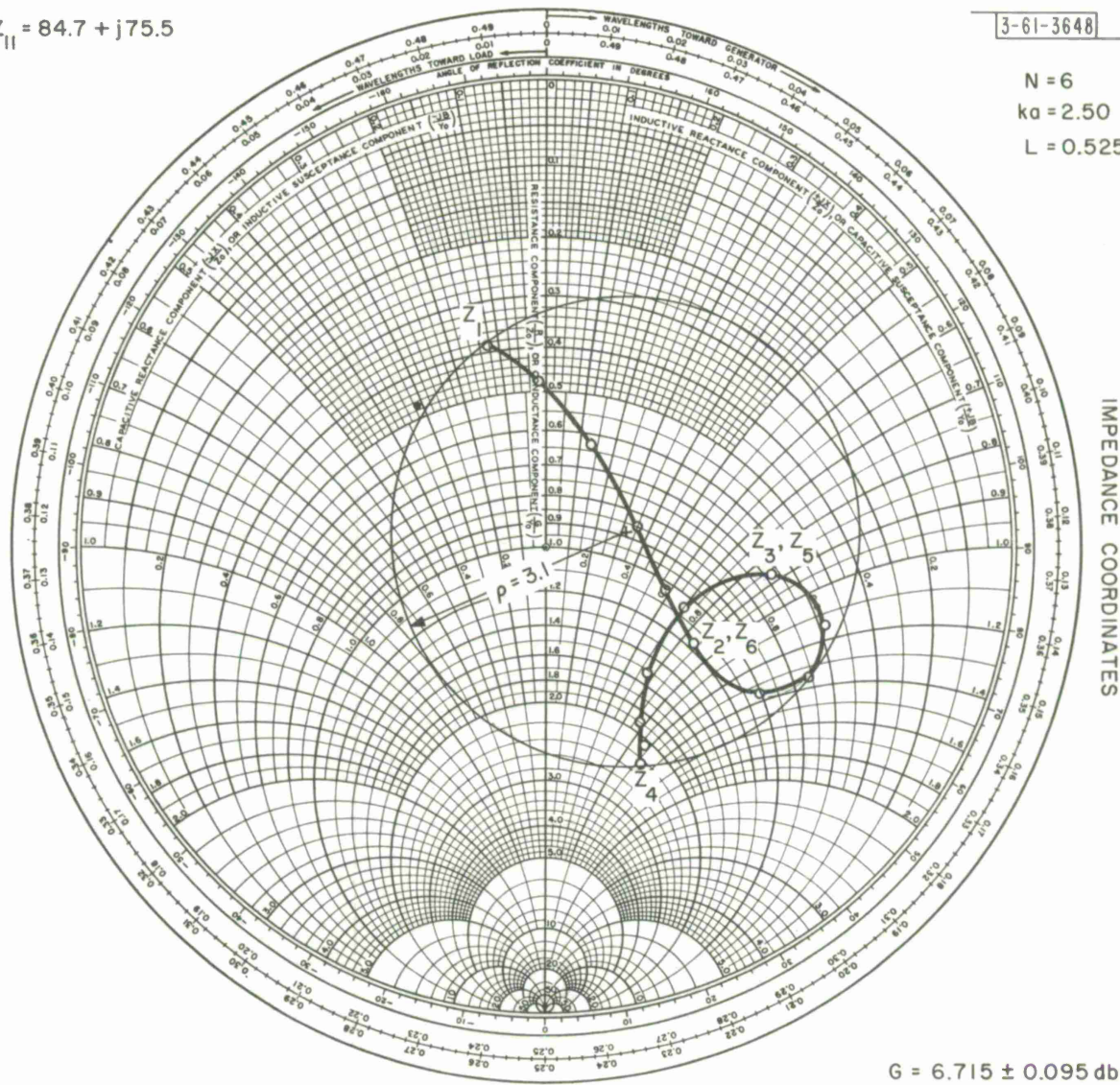
G = 6.715 ± 0.095 db

Fig. 11-e. Ring array impedance.

$$Z_{11} = 84.7 + j75.5$$

3-61-3648

N = 6
ka = 2.50
L = 0.525



$$G = 6.715 \pm 0.095 \text{ db}$$

Fig. 11-f. Ring array impedance.

$$Z_{11} = 73.1 + j42.5$$

3-61-3649

N = 5
 $ka = 2.28$
 $L = 0.500$

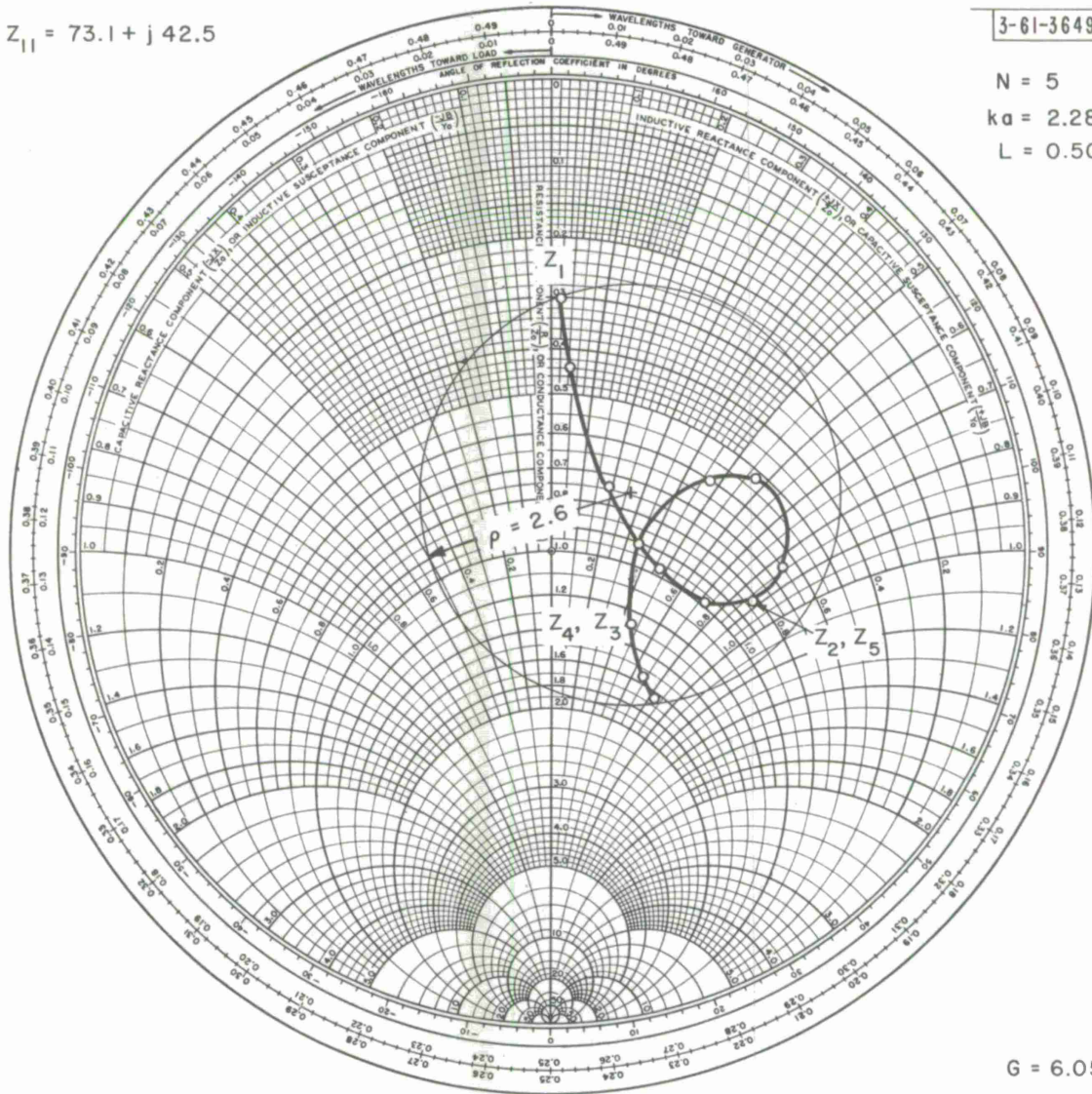


Fig. 11-g. Ring array impedance.

$$Z_{11} = 63.08 + j10.4$$

3-61-3650

N = 5
 ka = 2.28
 L = 0.475

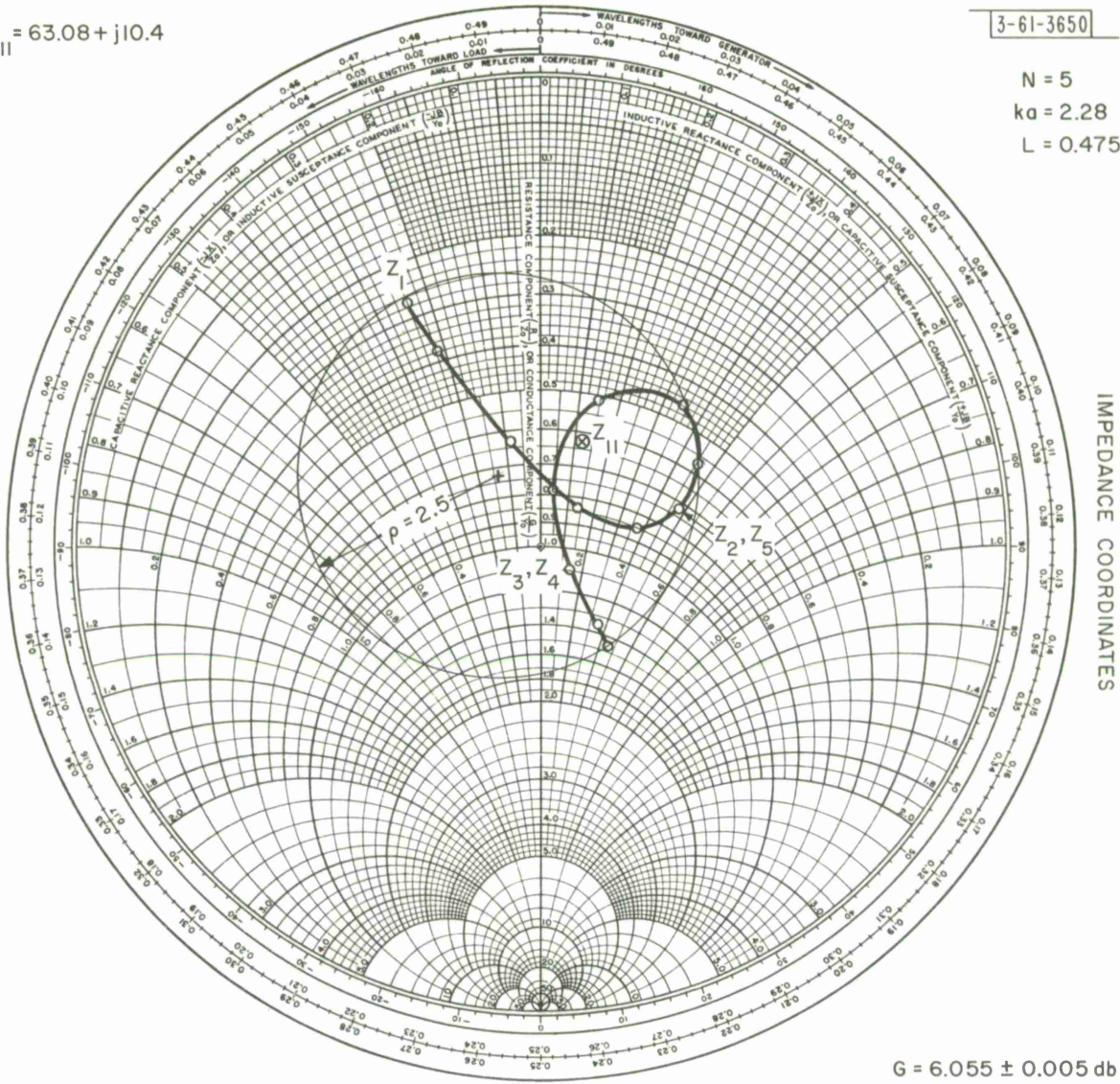
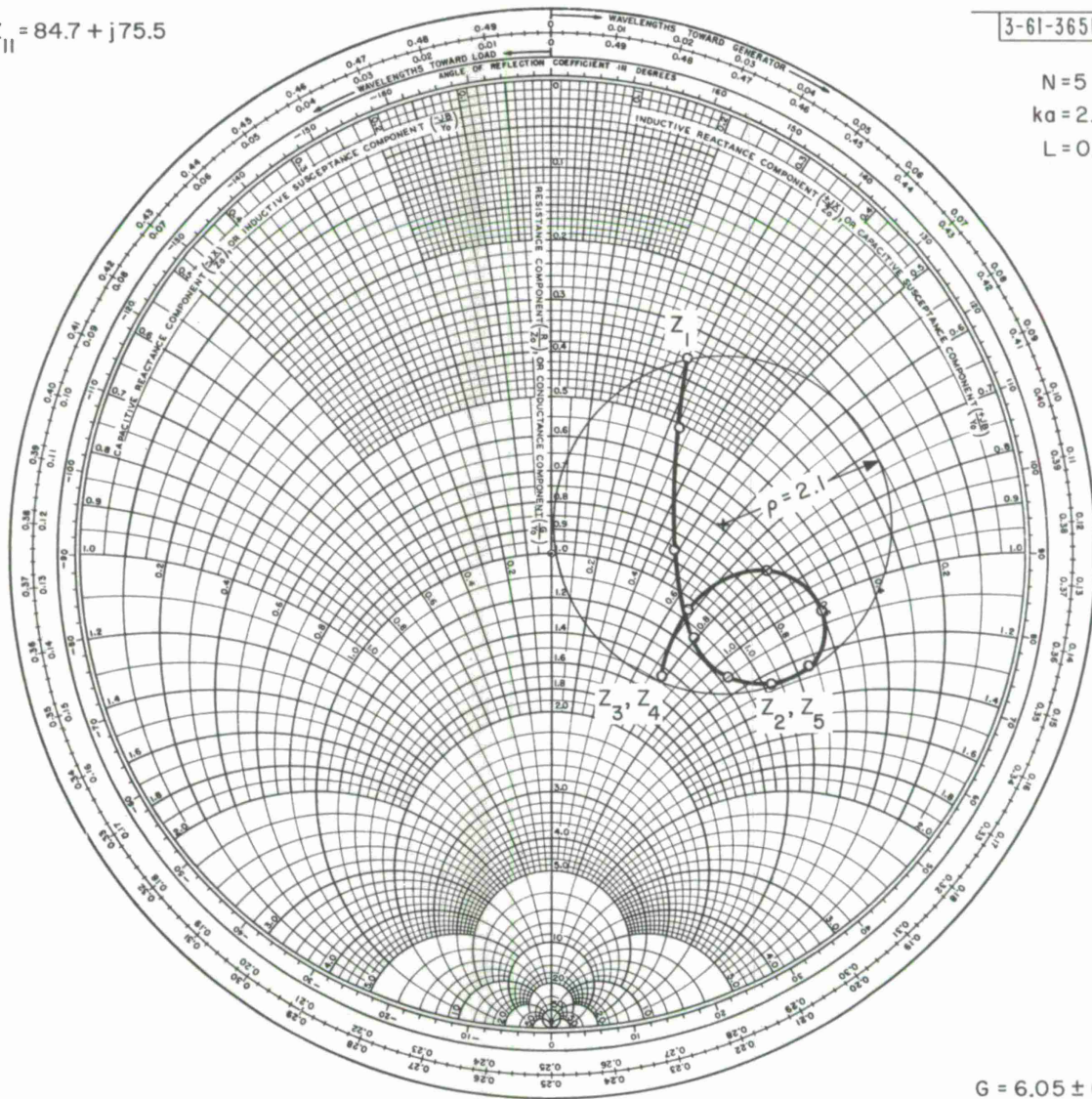


Fig. 11-h. Ring array impedance.

$$Z_{II} = 84.7 + j75.5$$

3-61-3651

$N = 5$
 $ka = 2.28$
 $L = 0.525$



IMPEDANCE COORDINATES

$G = 6.05 \pm 0 \text{ db}$

Fig. 11-i. Ring array impedance.

$$Z_{11} = 63.1 + j10.4$$

3-61-3652

$N = 5$
 $ka = 2.5$
 $L = 0.475$

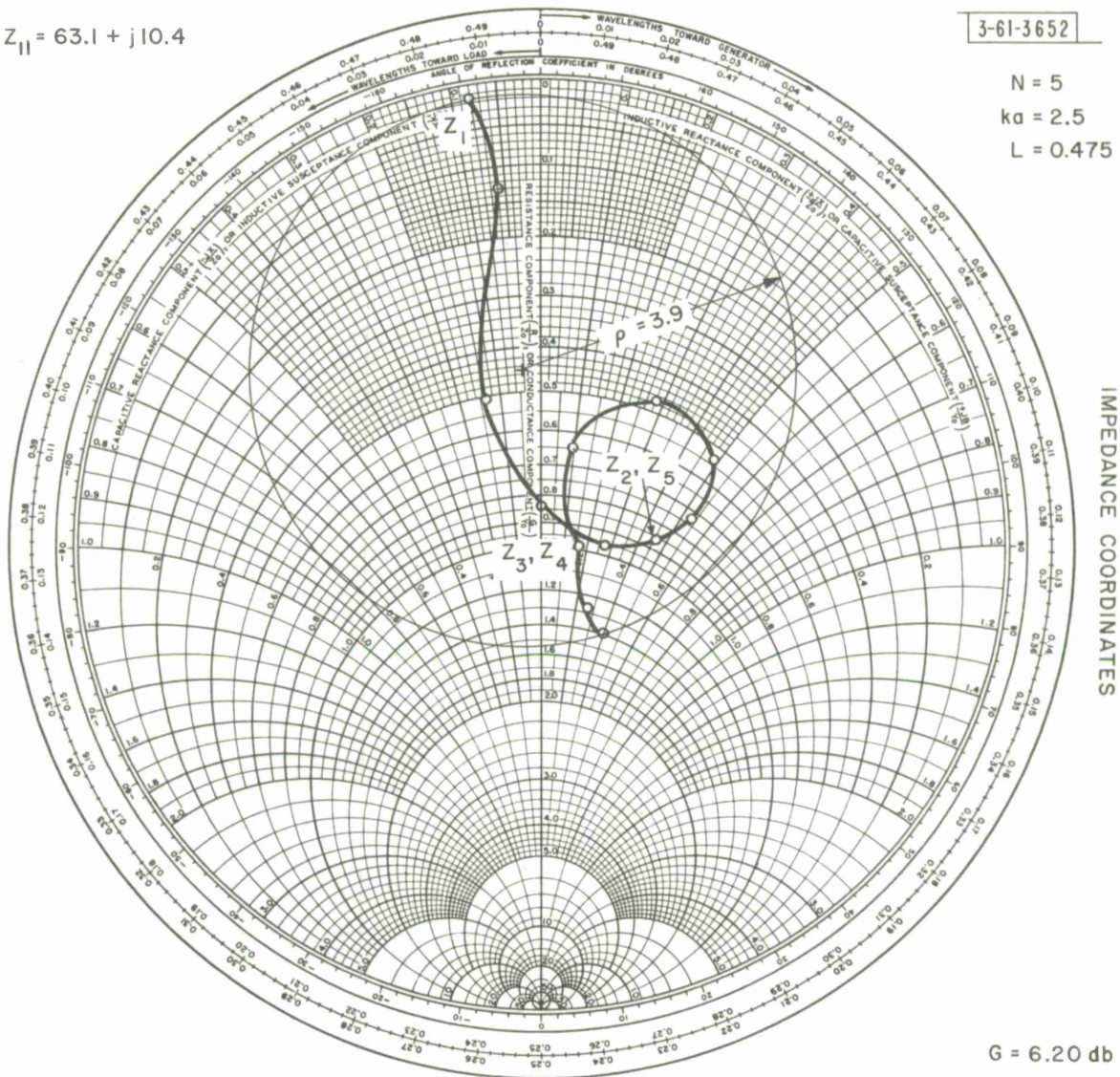
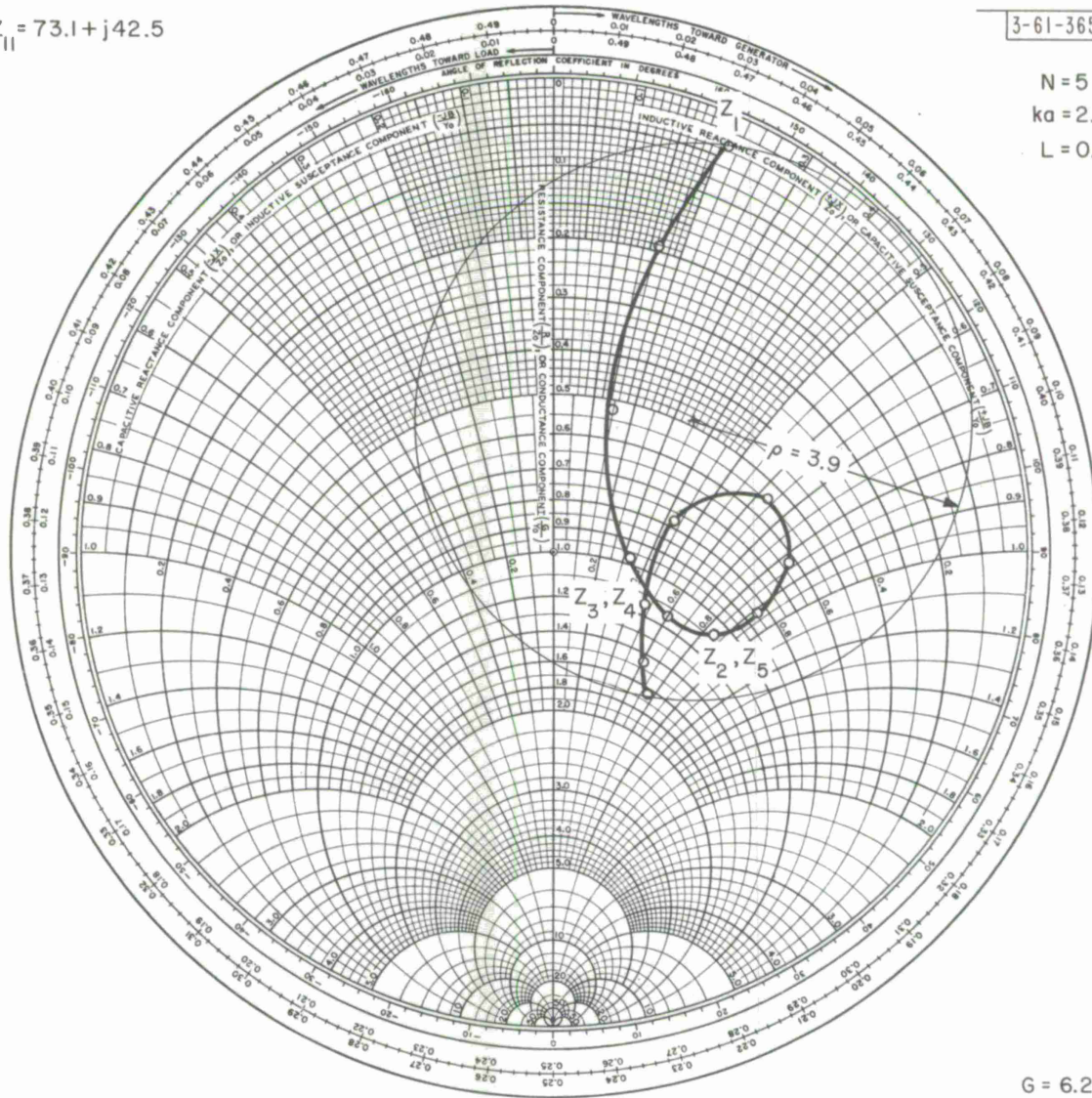


Fig. 11-j. Ring array impedance.

$$Z_{11} = 73.1 + j42.5$$

3-61-3653

$N = 5$
 $ka = 2.5$
 $L = 0.500$



$G = 6.20 \text{ db}$

Fig. 11-k. Ring array impedance.

$$Z_{11} = 63.1 + j10.4$$

3-61-3654

$N = 4$
 $ka = 2.28$
 $L = 0.475$

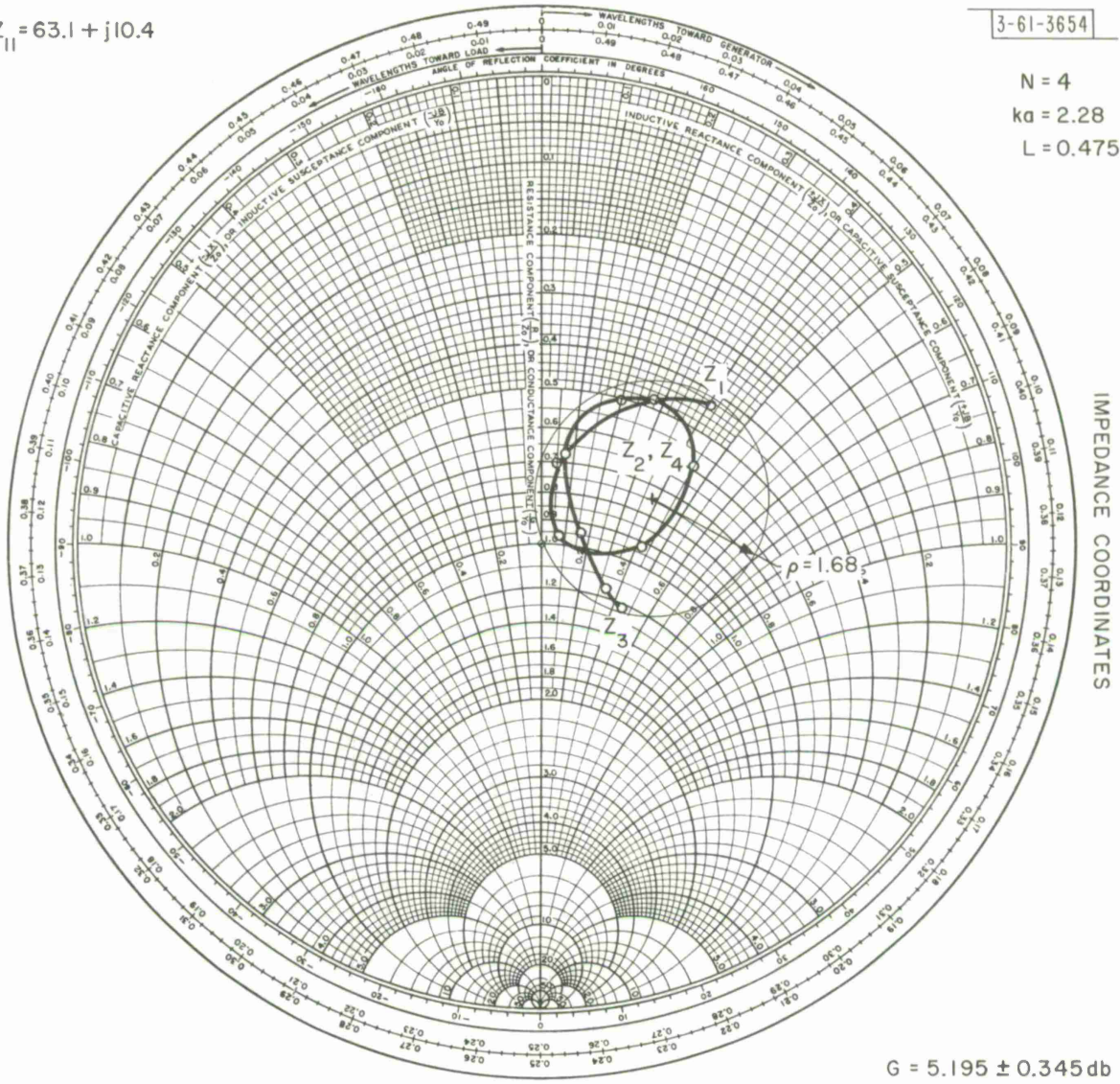
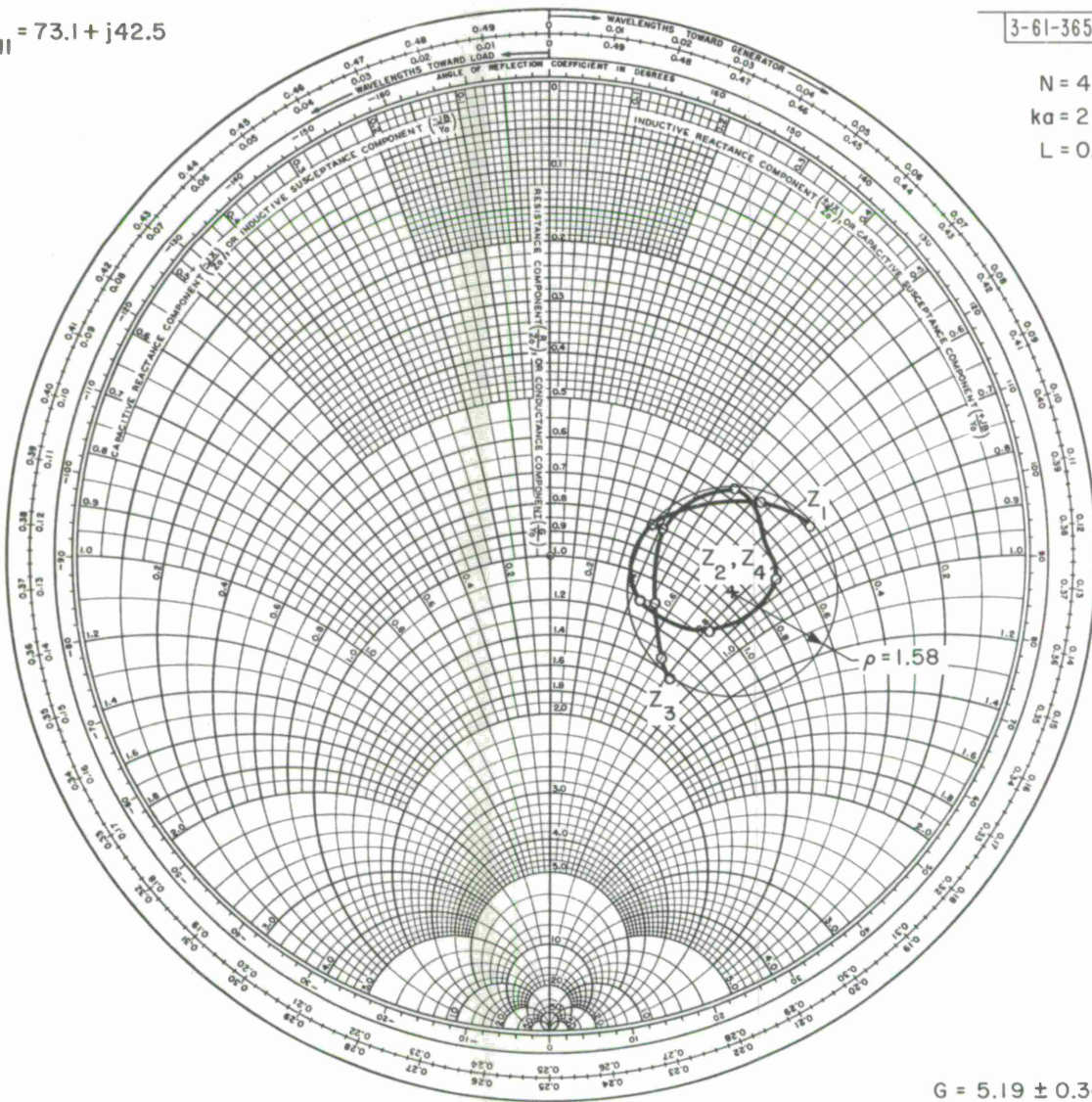


Fig. 11-1. Ring array impedance.

$$Z_{11} = 73.1 + j42.5$$

3-61-3655

$N = 4$
 $ka = 2.28$
 $L = 0.500$



$G = 5.19 \pm 0.34$ db

Fig. 11-m. Ring array impedance.

DISTRIBUTION LIST

Division 6

Dinneen, G. P.
Morrow, W. E.

Group 61

Ricardi, L. J. (20)
Assaly, R. N.
Burrows, M. L.
Crane, R. K.
Devane, M. E.
LaPage, B. F.
Lindberg, C. A.
Malbon, R. M.
Niro, L.
Peck, R. J.
Rankin, J. B.
Rosenthal, M. L.
Sotiropoulos, A.

Group 62

Rosen, P. (5)

Group 63

Sherman, H. (5)

Group 64

Green, P. E.

Group 65

Wood, R. V.

Group 66

Reiffen, B.

Division 3

Chisholm, J. H.
Ruze, J.

Division 4

Weiss, H. G.

Group 44

Allen, J. L.

Group 45

Ward, W. W.

Group 46

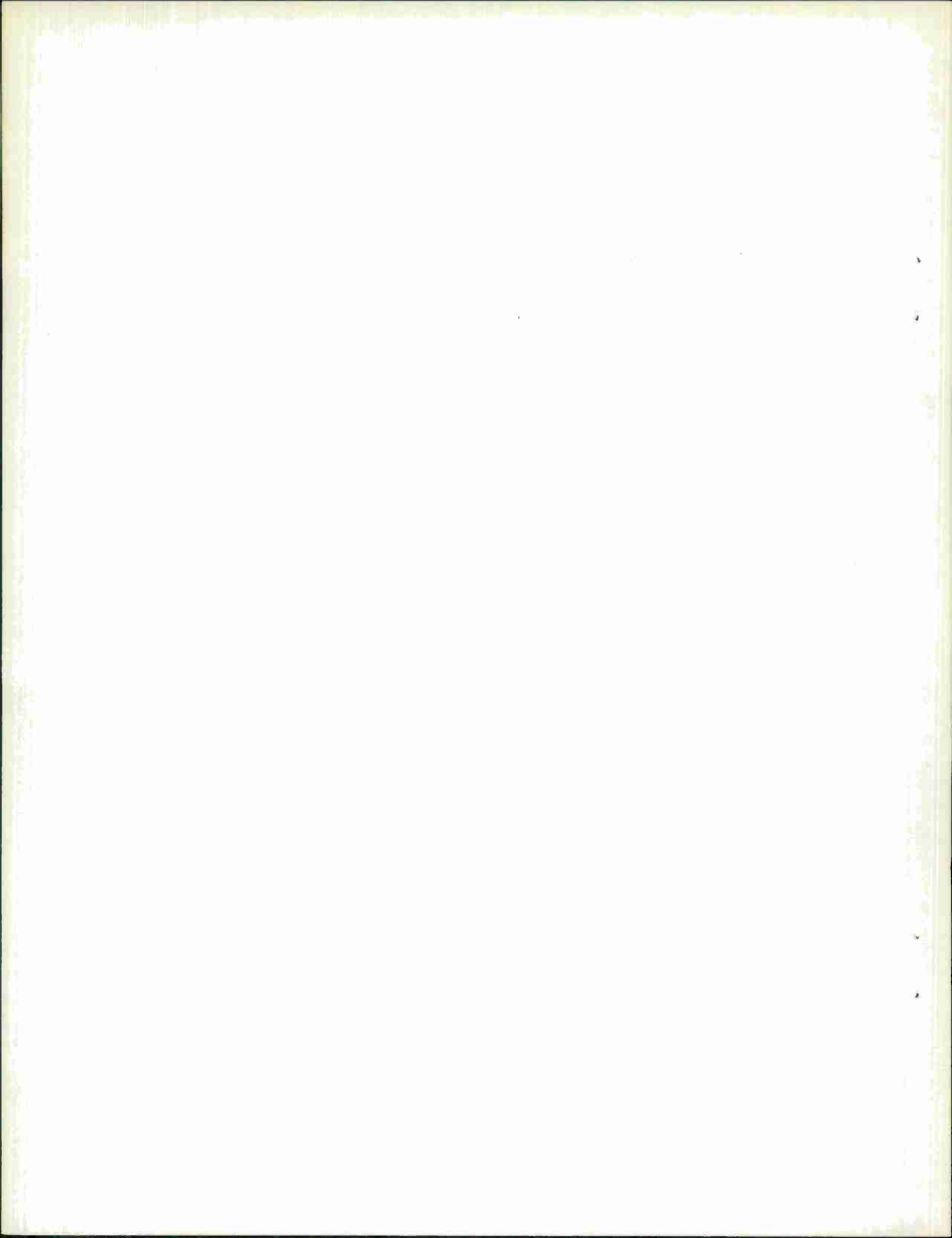
Jones, C. W.
Keeping, K. J.

Division 7

Hutzenlaub, J. F.

Group 71

Blaisdell, E. W.



Printed by
United States Air Force
L. G. Hanscom Field
Bedford, Massachusetts

